Applied Energy 363 (2024) 122977

Contents lists available at ScienceDirect

Applied Energy

journal homepage: www.elsevier.com/locate/apenergy

Modeling the impact of extreme summer drought on conventional and renewable generation capacity: Methods and a case study on the Eastern U.S. power system

Hang Shuai [a], Fangxing Li [a,*], Jinxiang Zhu [b], William Jerome Tingen II [a], Srijib Mukherjee [c]

[a] Department of Electrical Engineering and Computer Science (EECS), The University of Tennessee at Knoxville (UTK), 1520 Middle Drive, Knoxville, 37996, TN, USA

[b] Hitachi Energy, 901 Main Campus Drive, Raleigh, 27606, NC, USA

[c] Energy Science and Technology Directorate, Oak Ridge National Laboratory (ORNL), P.O. Box 2008, Oak Ridge, 37831, TN, USA

GRAPHICAL ABSTRACT

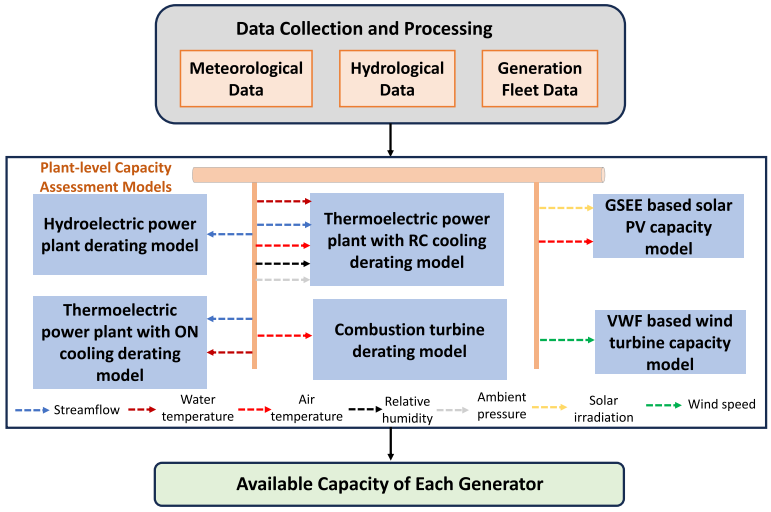

- A comprehensive and systematic framework for assessing the impact on generating capacity in bulk power systems during summer droughts is developed.
- The proposed approach is applied in the PJM and SERC regions of the United States, encompassing a total of 6,055 at-risk generators.

ARTICLE INFO

Keywords:
Power system resilience
Drought
Generating capacity
Extreme weather
Climate change

ABSTRACT

Across recent years, there has been a growing prevalence of extreme weather events throughout the United States, posing significant challenges to the reliable and resilient operation of power systems. Specifically, summer droughts threaten to severely reduce available generation capacity to meet regional electricity demand, potentially leading to power outages. This underscores the importance of accurate resource adequacy (RA) assessment to ensure the reliable operation of the nation's energy infrastructure. Accurately evaluating the usable capacity of regional generation fleets is a challenging undertaking due to the intricate interactions between power systems and hydro-climatic systems. This paper proposes a systematic and analytical framework

* Corresponding author.
E-mail address: fli6@utk.edu (F. Li).

https://doi.org/10.1016/j.apenergy.2024.122977
Received 7 November 2023; Received in revised form 25 January 2024; Accepted 2 March 2024
Available online 27 March 2024

to evaluate the impacts of extreme summer drought events on the available capacity of various generating technologies, incorporating both meteorological and hydrologic factors. The framework provides detailed plant-level capacity derating models for hydroelectric, thermoelectric, and renewable power plants, facilitating evaluations with high temporal and spatial resolution. The application of the proposed impact assessment framework to the 2025 generation fleet of the real-world power system within the PJM and SERC regions of the United States yields insightful results. By analyzing the daily usable capacity of 6,055 at-risk generators across the study region, it shows that the summer capacity deration is most significant for hydroelectric and once-through thermal power plants, followed by recirculating thermal power plants and combustion turbines. In the event of the recurrence of the 2007 southeastern summer drought event in the near future, the generation fleet could experience a substantial reduction in available capacity, estimated at approximately 8.5 GW, compared to typical summer conditions. The sensitivity analysis reveals that the usable capacity of the generation fleet would suffer an even more significant decrease under conditions of increasingly severe summer droughts. The proposed approach and the findings of this study provide valuable methodologies and insights, empowering stakeholders to bolster the resilience of power systems against the potentially devastating effects of future extreme drought events.

Nomenclature

Abbreviations

CT	Combustion turbine
EI	Eastern Interconnection
ON	Once-through cooling
PJM	Pennsylvania-New Jersey-Maryland
PV	Photovoltaic
QC	Qualified capacity
RA	Resource adequacy
RC	Recirculating cooling
$SERC$	Southeastern Electric Reliability Council
VRE	Variable renewable energy
WT	Wind turbine

Physics constants

ρ_a	Density of air (kg/m^3)
ρ_w	Density of water (kg/m^3)
$C_{p,w}$	Heat capacity of water (MJ/kg °C)
g	Gravity acceleration constant (m/s^2)
K	Psychrometer constant

Parameters

ΔTl^{max}	Maximum permissible water temperature rise through the condenser (°C)
η_{net}	Net efficiency of generator
γ	Maximum fraction of water flow available for cooling power plant (%)
σ	Water-air mass flow ratio (%)
c_T	PV module temperature coefficient
c_{ct}	Power-temperature coefficient of combustion turbine
h_{fg}	Latent heat of vaporization of water (MJ/kg)
H_{net}	Net hydraulic head acting on the turbine (m)
k_{os}	Fraction of heat not removed by cooling system
n_{cc}	Cycles of concentration
P_n	Rated capacity of generator (MW)
T_{app}	Difference between ambient wet bulb temperature and the temperature to which water is actually cooled in cooling tower
Tl^{max}	Maximum permissible water temperature discharged to rivers (°C)
W_{on}	Water withdrawals when thermal plant operates at rated capacity

Subscripts/Superscripts

g	Generator category index
i	Generator index
max	Maximum value
t	Time index

Variables

ω_{out}, ω_{in}	Humidity ratio of air exiting and entering cooling tower, respectively
CF_g	Available capacity percentage of category g
G	Dry air mass flow rate (m^3/s) of cooling air into tower
$h_{a,out}$, $h_{a,in}$	Enthalpies (MJ/kg) of hot air leaving cooling tower and air entering cooling tower, respectively
H_{load}	Heat load of condenser (MJ/s)
h_{mu}, h_{bd}	Enthalpy (MJ/kg) of the makeup water and blowdown water, respectively
I	PV panel in-plane irradiance (W/m^2)
k_{sens}	Fraction of heat load that is transfer from liquid water to air (not by evaporation)
P_h	Available capacity of hydroelectric plant (MW)
p_w	Vapor pressure
P_{ct}	Available generating capacity of combustion turbine
P_{on}	Available capacity of thermal plant with ON cooling (MW)
P_{pv}	Ream-time PV power output
P_{rc}	Available capacity of thermal plant with RC cooling (MW)
P_{STC}	PV power output at standard test conditions (STC)
p_{tot}	Total ambient pressure
p_{ws}	Saturated vapor pressure

Q	Real-time flow rate of water (m^3/s)
T_c	Temperature of cooling water entering condenser (°C)
T_d	Dry-bulb air temperature (°C)
T_w	Inlet water temperature (°C)
T_{mod}	PV module temperature (°C)
T_{mu}	Temperature of makeup water (°C), which is equal to the temperature of inlet water from nearby river
W_{circ}	Flow rate (m^3/s) of water circulating through condenser of RC cooling systems
W_{evap}, W_d	Mass flow rate (m^3/s) of evaporation water and drift water losses, respectively
W_{mu}, W_{bd}	Mass flow rate (m^3/s) of makeup water and blowdown water, respectively

1. Introduction

1.1. Background

Extreme weather events (such as droughts [1,2] and hurricanes [3]) have exerted substantial and far-reaching effects on agriculture, water resources, energy systems, and the overall well-being of nations across the world. One illustrative case was the severe and enduring drought that afflicted the Southwestern United States across 2012–2017, which left an indelible impact on the region's ecosystems and society, as water usage was forced to be heavily restricted [4]. Even more recently, July 2023 experienced the highest global temperature ever recorded [5]. Recent research [6] indicates an alarming trend: the projected tenfold intensification of compound extreme heat and drought events on a global scale, which will pose significant challenges to the reliability and resiliency of power systems in meeting electricity demand [7–9]. For instance, a recent reliability assessment study by the North American Electric Reliability Corporation (NERC) found that the U.S. power grid to be at risk of outages during more extreme summer conditions [10]. In light of this, thoroughly understanding the pathways and quantifying the impacts of extreme drought on the power system is paramount to equip stakeholders with the necessary insights and preparedness required to tackle future extreme drought events.

To ensure the reliability and resiliency of power systems, stakeholders need to conduct resource adequacy (RA) assessments, which involve an in-depth analysis of the ability of generation resources to consistently meet energy demand, even under extreme conditions. An RA assessment comprises two fundamental steps: (1) quantifying the available usable capacity of generators and demands in a system and (2) calculating reliability and resilience metrics for a predefined time horizon. A major driver of generation resource availability is weather. This is primarily due to the profound impact that weather conditions can exert on the power generation of wind, solar photovoltaic (PV), hydro, or thermal, although the specific mechanism can vary. The RA analysis requires not only an understanding of the distributions of the weather conditions that drive resource availability, but also the correlations between them, which can be challenging to appropriately account for even in systems with a confined geographic scope [11]. The complexity is further magnified when accounting for all relevant correlations across expansive power systems, such as the Eastern United States. In this extensive region, different geographical areas exhibit different meteorological conditions, and the region's weather-sensitive power infrastructure, whether wind farms or thermal power plants, varies widely. To simplify the assessment process, the current practice of RA assessment in the United States [10,12,13] utilizes historical data to evaluate potential available generation capacity. For instance, the adoption of seasonal capacity factor or Seasonal Qualified Capacity (QC) [14], a de-rating factor derived from electricity production history, is a common approach to indicate the maximum power during a specific season. In numerous state-of-the-art power system reliability assessment tools, like GridLAB [15], historical generation data is employed as well to ascertain the usable capacity of generation fleets. However, this approach can have several drawbacks, such as potentially failing to explicitly reflect the available generation resources under specific extreme weather conditions that deviate from historical weather patterns. Additionally, correlations between the available capacities of different generators may not adequately be accounted for. Therefore, the integration of meteorological and hydrologic data and models into the RA assessment process is crucial for accurately characterizing the available capacity of a region. Accordingly, this work aims to address this gap by designing a bottom-up framework to systematically model the impact of extreme weather conditions on the available capacity of different generating units.

1.2. Previous work on generator capacity derating approaches

Droughts can vary in intensity and duration, but they often result in water shortages and impact the normal operation of power systems. The potential consequences of severe drought on hydroelectric power generation are noteworthy, potentially leading to constrained electricity supplies and elevated prices. For example, the historic drought that swept across much of the Western United States in 2021 resulted in a significant 48% decline in hydropower generation compared to the 10-year average [16]. In addressing these concerns, researchers have introduced various assessment approaches to quantify the impact of drought on hydroelectric generation, such as in [17–19]. These approaches rely on the hypothesis that annual generation of a hydro plant is proportional to annual flow within a basin. While this assumption holds a degree of validity, supported by a robust historical correlation between annual water flow and generation, the impact models utilized in these studies exhibit limitations, particularly concerning their spatial and temporal resolutions. For example, in terms of spatial resolution, the model presented in [17,18] simplifies the assessment by applying a uniform derating factor to the annual total generation of all hydro plants within a basin. In reality, basins typically host multiple hydro plants drawing water from diverse river sources. Therefore, the reduction in water flow ratios across these various rivers can vary, resulting in differing capacity derations depending on where the particular hydro plant is sited. Considering the linear relationship between average annual hydroelectric generation and average annual streamflow, the linear regression method is also a commonly used approach by researchers [20]. For a more precise assessment of the impact of drought on hydro plants, a commonly employed approach involves evaluating the individual plant's available generation capacity. This evaluation typically relies on a combination of factors such as exact plant location, plant capacity, hydraulic head, streamflow, and other relevant parameters, as discussed in previous studies [21,22]. It is worth noting that such modeling processes demand access to comprehensive datasets on these plants, ideally those that are publicly accessible [23].

Drought events can also significantly impact thermoelectric power plants, as highlighted in a study by Ref. [24]. A notable illustration is the prolonged drought that affected the Southeastern United States in 2007–2008, posing substantial risks to the operation of large baseload thermoelectric generation facilities within the region. Remarkably, as of 2021, thermoelectric power plants accounted for a significant 73% of the utility-scale electricity generated in the United States [25]. During drought events, the usable capacity of water-dependent thermoelectric power plants, such as coal-fired and nuclear facilities, can be significantly impacted by elevated water temperatures and restricted water availability. Additionally, air-cooled plants, such as combustion turbines, experience reductions in usable capacity due to the elevated

ambient air temperatures associated with drought conditions. To assess the impacts of drought on these plants' generation, a simplified methodology can been utilized by assuming that the reduction in generation at risk is directly proportional to the shortfall in cooling water flow experienced during the drought period relative to the total basin water demand in a normal year, as outlined in the studies by [18,26]. However, this simplified generation derating model may lack the precision required to accurately quantify the specific impact on an individual thermoelectric power plant. Alternatively, researchers have recently proposed an impact modeling approach based on regression analysis to assess the unit-level monthly average generation capability of fossil fuel units in the Western United States under drought conditions, as discussed in [27]. While this approach can achieve relatively higher spatial resolution in terms of generation deration, its temporal resolution is limited to a monthly basis, which may not adequately capture the finer details of drought impact on generators. For a more advanced and nuanced impact analysis, thermodynamic modeling can be employed. Depending on the cooling system, such as once-through (ON) [2] and recirculating (RC), employed by a given thermoelectric power plant, different thermodynamic modeling approaches can be adopted, as demonstrated in studies by [20,28,29]. These advanced modeling techniques offer a more tailored assessment of the effects of drought on individual power plants, accounting for their unique cooling configurations and operational characteristics. However, it is important to note that thermodynamic modeling approaches, while more accurate, are often only applied to a limited number of thermal plants in a localized area due to the complexity of the modeling process. For example, in [28,29], thermodynamic models were only employed to assess the impact of weather on the capacity of a single nuclear plant and 52 once-through plants, respectively.

Power systems are undergoing a rapid transformation, transitioning from conventional fossil fuel generation to renewable sources such as wind and solar. However, the understanding of how extreme weather events affect the available capacity of renewable energy sources, such as solar PV and wind turbines, remains relatively limited. This knowledge gap becomes particularly apparent in the context of summer droughts, which frequently align with elevated air temperatures. Regarding solar PV power generation, one of the most significant impacts of high temperatures is the derating of solar PV modules and DC-to-AC inverters, as discussed in the study by [30]. For wind turbines, the usable capacity of wind farms during summer droughts can be substantially affected by wind speed. This is especially pertinent since low wind events could occur during summer drought periods. As an illustrative example, Europe experienced an extended period of dry conditions and low wind speeds throughout the summer and early autumn of 2021 [31]. Therefore, it is imperative to include solar PV and wind turbine capacity derating models when assessing the available capacity of a power system's generation fleet under summer drought conditions. This ensures a more comprehensive evaluation of the system's resilience in the face of dynamic climate conditions and evolving energy sources. The aforementioned studies (such as [26,27,32]) notably lacked capacity models for solar PV and wind systems, precluding a comprehensive assessment of the holistic impact of drought events on the available capacity of generation fleets. This absence of consideration for solar PV and wind capacity modeling represents a notable research gap in the existing literature within the realm of power system drought event impact analysis.

1.3. Significance of this research

Through an analysis of historical data spanning from 1940 to 2023, researchers discovered that 19 out of the 30 hottest months on record globally occurred within the last eight years [33]. This trend underscores the urgent need for a comprehensive investigation into impacts of drought events on the capacity of generation fleets in the US power systems. Accordingly, the Federal Energy Regulatory Commission (FERC) is currently formulating how to best direct NERC on handling the impact of extreme drought-induced reductions in the supply side within the bulk power system planning process, specifically by developing modifications to Reliability Standard TPL–001–5.1 [34]. This research gap is particularly pronounced within the Eastern Interconnection (EI) system, where a significant number of conventional power plants are expected to remain operational in the foreseeable future. Therefore, a thorough and methodical assessment of drought impacts on the generation resources in the near-term is crucial.

In the U.S. power industry [10,35], the capacity of both conventional and renewable power plants under normal weather conditions is commonly derated using historical resource performance data. This includes methods such as employing the (90/10) point of the resource performance distribution or utilizing Seasonal QC data. While these capacity derating methods are straightforward to apply, they are characterized by low temporal and spatial resolution, failing to explicitly capture the impacts of weather conditions on individual generators within the study region. In other words, derating based on historical performance data cannot accurately reflect the actual impacts of an extreme drought event that has not previously occurred. Additionally, these methods inadequately address the correlations between the weather-dependent available capacities of various generators.

This research sheds light on a significant gap in the field — the lack of a comprehensive and systematic framework for evaluating the impact on generating capacity in bulk power systems during summer drought, particularly one that provides both high temporal and spatial resolution across various generating technologies. This gap is noteworthy considering the EI is one of the largest power systems globally, boasting a substantial capacity of 700 GW [36]. Despite its importance, a thorough understanding of the effects of extreme summer drought on generation capacity within the EI system has not been adequately explored. This research is crucial for advancing the understanding of the EI system reliability and resilience in the face of evolving climate challenges.

1.4. Contributions and specific objectives

This paper aims to bridge the aforementioned research gap by introducing a systematic framework for summer drought impact evaluation, which boasts both high temporal and spatial resolution across a range of generating technologies. The objective is to establish a precise methodology for assessing the deration of generating capacity, thereby offering insights into the usable capacity of various generating technologies within the EI system when confronted with extreme drought conditions. This study specifically addresses the following questions:

1. To what extent would summer drought impact the near-term available generating capacity of hydro, thermal, and variable renewable energy (VRE) fleets in the EI system?
2. How sensitive is the near-term available generating capacity of the EI system to variations in extreme temperature and streamflow during summer drought events?

The main contributions are summarized as follows:

- This paper introduces a comprehensive and systematic framework for evaluating the impact on generating capacity in bulk power systems during summer droughts. This framework is meticulously designed to assess the usable generating capacity at the plant level, covering various generating technologies such as hydro, thermal (once-through cooling, recirculating cooling, or dry cooling), and VRE, all using a daily time resolution. It features advanced plant-level VRE capacity evaluation models to accurately gauge the impact of summer droughts on the usable capacity of solar PV and wind turbines. The proposed method holds the advantage of assessing the impacts on the generating

capacity of generation mix over a wide geographical area with a high temporal and spatial resolution. It also takes into account the correlations between the available capacities of different generators.

- This research offers valuable insights into the usable capacity of various generating technologies in the EI system under extreme drought conditions. The approach is applied to the real-world power systems within the Pennsylvania-New Jersey-Maryland (PJM) and Southeastern Electric Reliability Council (SERC) regions in the United States, covering 6055 at-risk generators. To the best of the authors' knowledge, this is the first paper that provides quantitative evaluations showing the tangible effects of historical summer drought on the available generation capacity of the near-term PJM and SERC generation fleet. The outcomes of this evaluation are significant, offering crucial insights and serving as an invaluable methodology for stakeholders. The findings enable stakeholders to better prepare and strategize for future extreme drought scenarios.

The following sections present: (1) description of the impact modeling framework, which includes the methods to evaluate available capacity of different generating technologies; (2) assessing results of the study region; (3) conclusion and discussion of the impacts of extreme drought events on the bulk power system.

2. Systematic framework for assessing the impact of summer drought on generating capacity

This section presents a framework designed to evaluate the impact on generating capacity during extreme drought conditions. It also provides detailed modeling methodologies specifically designed for a diverse range of power generation technologies. These include hydroelectric generators, thermoelectric power plants with once-through cooling systems, thermoelectric power plants with recirculating cooling systems, combustion turbines, solar PV systems, and wind turbines.

2.1. Modeling framework

The systematic framework for assessing the impact on generating capacity in bulk power systems during summer droughts is illustrated in Fig. 1. The process can be summarized as follows: (1) Collection of meteorological and hydrological data during summer drought conditions, either by gathering real-world data or simulation as needed. Simultaneously, crucial information about power generators is compiled, including details such as their geographical location, installed capacity, generation techniques, the source of cooling water withdrawal, and various relevant parameters. (2) Application of plant-level capacity derating models to each at-risk power plant within the system, taking into account the specific characteristics of each plant and their vulnerability to drought conditions. (3) Analyzing the results obtained from these models, providing insights into the available generating capacity under the influence of summer droughts.

In the following subsections, the models utilized to quantify the impacts of summer drought conditions on the available capacity of hydro, thermal (with various cooling systems), solar PV, and wind turbines are presented.

2.2. Capacity derating for hydroelectric power plant

In the context of hydropower facilities, the primary determinant for generation is streamflow. Consequently, Refs. [17–19] determine hydro generation deration based on the hypothesis that annual generation of a hydro plant is proportional to annual flow within a given basin. The correlation between annual generation and flow rate can be demonstrated by examining historical state-level flow and hydro generation of the PJM and SERC regions, as depicted in Fig. 2, revealing a association between the two variables. Of the 15 states analyzed, five (AL, GA, NC, PA, and SC) showed a strong correlation between generation and flow, with fit values $R^2 > 0.7$. But, four states (IL, IN, OH, and WV) exhibited notably poor correlations, where $R^2 < 0.3$. Several factors contribute to the weak correlations observed in some states, including limitations on generation capacity during high-flow periods, the release of reservoir storage during low-flow periods, and the competing demands for reservoir resources such as fish, water supply, and flood control. According to the analysis, relying solely on annual reductions in flow to derate the generation capability of hydroelectric plants within a region, as suggested in the study by Ref. [18], is an imprecise approach. Moreover, the model simplifies by uniformly applying a derating factor to all hydro plants in a basin, without accounting for variations in water flow among different plants within the same basin.

To assess the impact of drought on hydroelectric plants with greater precision, this study employs a plant-level analytical generating capacity derating model. The daily generating capacity of the ith hydroelectric power plant is determined based on the real-time flow rate of water passing through the turbine, as expressed by the following equation:

$$P_{h,i} = min\left\{ \frac{\eta_{net,i} \cdot \rho_w \cdot Q_i \cdot g \cdot H_{net,i}}{1000000}, P_{n,i} \right\} \quad (1)$$

The equation shows that the usable capacity of a specific hydroelectric power plant is dependent on the available water flow. Therefore, the daily available water flow has a significant impact on the generation capacity of hydroelectric plants.

To employ Eq. (1) for modeling the impact of drought on the available capacity of hydropower plants, it is necessary to gather plant-level streamflow data and plant-specific parameters, including installed capacity, dam height, and other relevant factors. In the PJM and SERC regions, there will be a total of 773 hydro generators operating by the summer of 2025, taking into account both retired hydro units before the summer of 2025 and newly added hydro generators before the same time. To calculate the daily usable capacity of each hydroelectric power plant under different summer drought scenarios utilizing Eq. (1), the historical daily streamflow data can be gathered from the United States Geological Survey (USGS) water information dataset [37]. If the historical data of specific surface-water sites is missing, historical meteorological data and hydrological models can be utilized to simulate the daily streamflow of all rivers in the PJM and SERC regions. The hydraulic height information of each hydroelectric power plant was extracted from the NID database [38]. The efficiency of all hydroelectric power plants is assumed to be 90%. The information about the hydroelectric power plants, including their names, installed capacities, locations, retirement years, etc., was collected from Form EIA-860M (2022 version) [39]. The process to calculate the usable capacity of conventional hydroelectric power plants is presented in Algorithm 1.

Algorithm 1 Conventional hydroelectric power plant generation capacity evaluation algorithm

Input: Hydroelectric plant information; Streamflow of each power plant.

Output: Daily available capability of each hydroelectric power plant.

```
for Every hydroelectric power plant do
    Get the location, installed capacity P_{n,i}, hydraulic head H_{net,i}, generation net efficiency η_{net,i} information of the ith conventional hydroelectric power plant;
    for Every time step do
        1) Obtain the real-time streamflow value (Q_i^t) at the plant's location;
        2) Based on equation (1), calculate the daily usable capacity of the plant;
    end for
end for
```

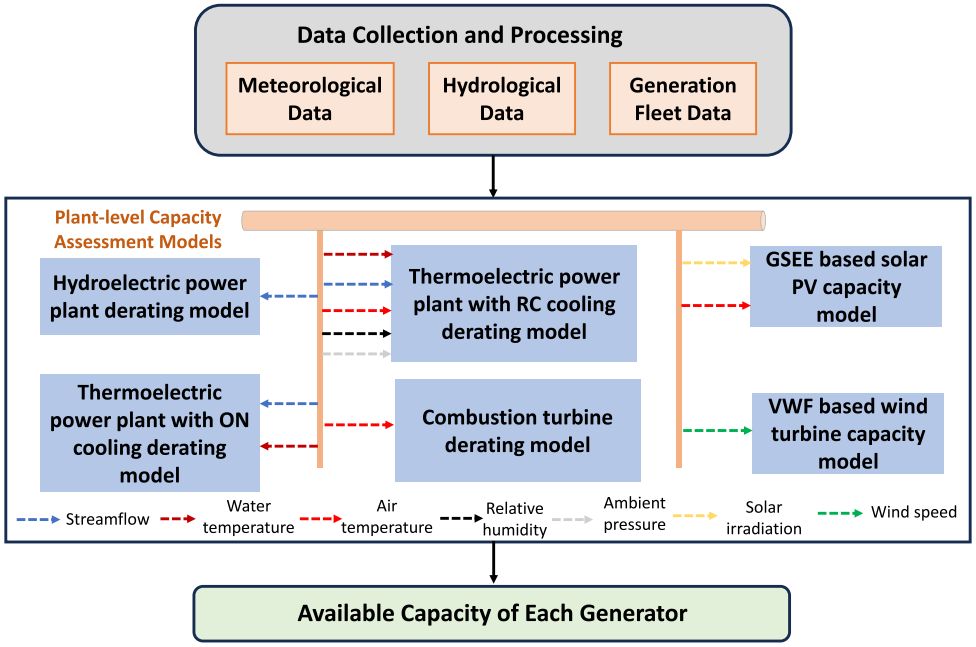

Fig. 1. Proposed framework for assessing the impact on generating capacity in bulk power systems during summer droughts.

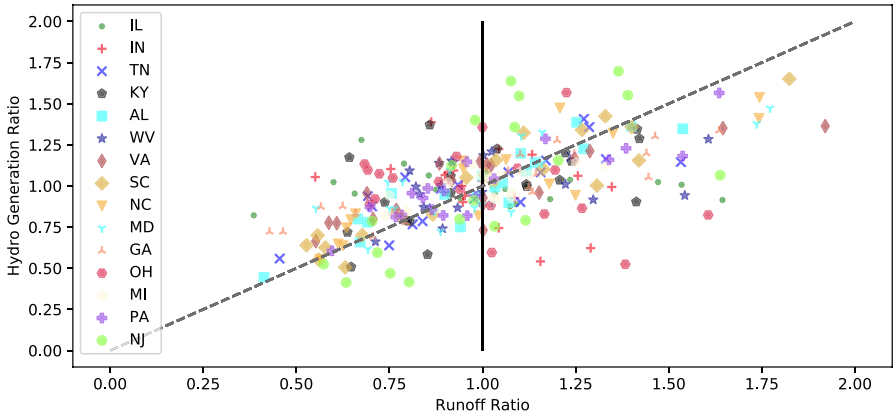

Fig. 2. Correlation between water flow and the hydroelectric generation for each state. Each data point represents a single year between 2001–2020. The flow ratio (annual flow/average flow) is on the x-axis and the generation ratio (annual generation/average generation) is on the y-axis. If the assumption of annual generation is proportional to annual flow fits the data points perfectly, it would expect all of the data points to line up exactly on the dashed black line which shows where the flow ratio is exactly equal to the generation ratio.

2.3. Capacity derating for thermoelectric power plant with once-through cooling system

For once-through cooling systems, where water is withdrawn for cooling and then immediately deposited back in the river after one cycle, plant usable capacity is mainly constrained by the availability of water (streamflow) and water temperatures. According to Ref. [29], the maximum usable capacity of the ith once-through thermoelectric power plant, $P_{on,i}$ (MW), can be computed using the following equation:

$$P_{on,i} = \frac{\min(\gamma \cdot Q_i, W_{on,i}) \cdot \rho_w \cdot C_{p,w} \cdot \max(\min(Tl^{max} - T_{w,i}, \Delta Tl_i^{max}), 0)}{\frac{1-\eta_{net,i}-k_{os,i}}{\eta_{net,i}}} \tag{2}$$

where $W_{on,i}$ is the water withdrawals when the plant operates at rated capacity $P_{n,i}$, which can be calculated as follows:

$$W_{on,i} = P_{n,i} \cdot \frac{1-\eta_{net,i}-k_{os,i}}{\eta_{net,i}} \cdot \frac{1}{\rho_w \cdot C_{p,w} \cdot \max(\min(Tl^{max} - T_{w,i}, \Delta Tl_i^{max}), 0)} \tag{3}$$

All operating and planned once-through thermoelectric power plants in the PJM and SERC regions were identified based on cooling system information provided in Form EIA-860 (2022 version). Previous research has indicated that once-through thermoelectric power plants using fresh surface water to cool the plants are considered at-risk during summer drought events, while those using ocean water, ground water, and other sources are considered low-risk [18]. There are a total of 137 at-risk once-through thermoelectric power generators in the study region, and information on these plants is available upon request. To compute the daily usable capacity of each at-risk once-through thermoelectric generator under drought scenarios, historical daily streamflow (Q_i) and water temperature ($T_{w,i}$) data can be gathered from the USGS water information dataset [37]. If the historical data of specific sites is missing, the historical meteorological data and hydrological models can be used to simulate Q_i and $T_{w,i}$ for the generators. The process to calculate the usable capacity of once-through cooling thermoelectric power plants is presented in Algorithm 2.

Based on median value of maximum permissible river water temperatures in the United States, Tl^{max} is set to 32 °C in this work. ΔTl_i^{max} is evaluated for each thermoelectric power plant using historical discharge average temperature and intake average temperature data from Form EIA-923 [40]. Similarly, installed capacity and net efficiency information of each plant is determined according to generator and plant data from Form EIA-860 and Form EIA-923. k_{os} is roughly 12% for coal-fired generators, and 20% for natural gas-fired generators [2]. The fraction of water available for withdrawal is usually determined using the method of Tennant [41]. In this work, γ is set to be 30% for summer seasons.

Some once-through thermoelectric power plants contain a steam turbine generator and another different type of generators. For example, combined cycle power plants are consist of combustion turbine generators and steam turbine generators. To account for the partial contribution of steam turbines to capacity derating of some once-through thermoelectric power plants, Form EIA-860 is used to determine the capacity contributed by each generator at each plant. The capacity reduction of the steam turbine generator is calculated according to the above equation (if once-through cooling system is utilized), while the capacity reduction of combustion turbine (CT) generator is determined separately. The method to calculate the capacity reduction of combustion turbine is introduced as follows.

Based on Eqs. (2) and (3), the daily usable capacity of at-risk once-through plants in the PJM and SERC regions can be calculated. Fig. 3 shows the calculated usable capacity of Brunner Island plant (unit 2) in Pennsylvania during 2012–2014, with and without considering the maximum discharge water temperature limit. By the results in Fig. 3(c)–(d), it can be found that the usable capacity of the unit reduces more when considering the water temperature discharge limit. For example, the usable capacity (with regulatory limit) was less than 50% during the period from 7/1/2012 to 9/30/2012 as the inlet water temperature approached 32 °C. However, if the regulatory limit is not considered, the usable capacity will be almost unaffected.

To further validate the capacity derating model, a comparison was performed between the computed usable capacity and the historical actual power output of the generator, drawing from the AMPD (Air Markets Program Data) [42] records during the specified time intervals. As shown in Fig. 3(c)–(d), the green line indicates the actual power output of the unit. It can be observed that the green line is almost always below the blue solid line, indicating that the actual power output did not violate the calculated usable capacity when regulatory limits were not considered, which validated the effectiveness of the derating model. However, during some extreme periods, particularly in the summer season, the actual power output exceeded the calculated usable capacity considering regulatory limits, suggesting that the power plant may not have strictly adhered to state regulations during those historical periods. In this paper, it is assumed that all plants will strictly comply with state regulations in the future.

2.4. Capacity derating for thermoelectric power plant with recirculating cooling system

Recirculating (RC) cooling systems remove heat by evaporating water, and the cooling water is repeatedly used during the cooling process. Therefore, recirculating cooling systems need much less water withdrawals compared to once-through cooling systems. To model the impact of drought conditions on recirculating cooling based power plants, the capacity derating model given below can be applied. The cooling performance of recirculating system is mainly affected by atmospheric conditions (for example, air temperature and humidity), and intake water temperature plays a relatively small role [20]. Although recirculating cooling systems re-use cooling water, water withdrawals are also required to make up water losses. The water losses include evaporation losses W_{evap}, blowdown losses W_{bd}, and drift losses W_d.

Algorithm 2 Generation capacity evaluation algorithm for thermoelectric power plant with once-through cooling

Input: Thermoelectric power plant information; Streamflow, water temperature, etc.

Output: Daily available capability of each thermoelectric power plant.

1: Identify all at-risk once-through cooling thermoelectric power plant according to the water source information;
2: **for** Every at-risk power plant **do**
3: Get the location, installed capacity $P_{on,i}$, net efficiency $\eta_{net,i}$, fraction of heat not removed by the cooling system $k_{os,i}$, maximum permissible water temperature rise through the condenser ΔTl_i^{max}, maximum permissible water temperature discharged to river Tl^{max} information of the ith once-through cooling thermoelectric power plant;
4: **for** Every time step **do**
5: 1) Acquire real-time streamflow Q_i^t value and water temperature $T_{w,i}^t$ at the location of the plant;
6: 2) Based on equations (2) and (3), calculate the daily usable capacity of the plant;
7: **end for**
8: **end for**

Evaporation losses and blowdown losses comprise the majority of makeup water requirements, as shown in Eq. (4).

$$W_{mu,i} \approx W_{evap,i} + W_{bd,i} \tag{4}$$

The evaporation losses can be calculated using the heat load of the condenser $H_{load,i}$ (MJ/s):

$$W_{evap,i} = \frac{H_{load,i} \cdot (1 - k_{sens,i})}{\rho_w \cdot h_{fg}} \tag{5}$$

where k_{sens} is the fraction of the heat load that is transfer from the liquid water to the air (not by evaporation). The value of k_{sens} is a function of incoming air temperature, humidity, and ambient air pressure. h_{fg} is the latent heat of vaporization of water, which is equal to 2.45 MJ/kg in this work. The blowdown losses can be calculated based on W_{evap} and the evaporation rate n_{cc}:

$$W_{bd,i} = \frac{W_{evap,i}}{n_{cc} - 1} \tag{6}$$

where n_{cc} denotes cycles of concentration, which ranges from 3 to 6. In this work, a typical value of 6 [20] is adopted.

The heat input to the tower include the heat from condenser and makeup water. The heat output form the tower include the energy of hot air leaving the tower and the energy of blowdown water. The heat balance in cooling tower can be expressed by Eq. (7).

$$H_{load,i} + \rho_w \cdot W_{mu,i} \cdot h_{mu,i} = \rho_a \cdot G_i \cdot (h_{a,out,i} - h_{a,in,i}) + \rho_w \cdot W_{bd,i} \cdot h_{bd,i} \tag{7}$$

Substituting Eq. (6) to (4), the following equation is obtained:

$$W_{mu,i} = \frac{n_{cc} \cdot W_{evap,i}}{n_{cc} - 1} \tag{8}$$

And the following mass balance equation is applicable:

$$\rho_w \cdot W_{mu,i} = \rho_w \cdot W_{evap,i} + \rho_w \cdot W_{bd,i} = \rho_a \cdot G_i \cdot (\omega_{out,i} - \omega_{in,i}) \tag{9}$$

The data on dry air mass flow rate G_i is rarely available. The above heat balance and mass balance equations can be solved by introducing the water-air mass flow ratio σ as follows:

$$\sigma = \frac{\rho_w \cdot W_{circ,i}}{\rho_a \cdot G_i} \tag{10}$$

The value of σ ranges between 0.5 and 1.5 with a typical value of 0.8. Using water circulating rate, the water losses can be reformulated as follows:

$$W_{mu,i} = \frac{W_{circ,i}}{\sigma}(\omega_{out,i} - \omega_{in,i}) \tag{11}$$

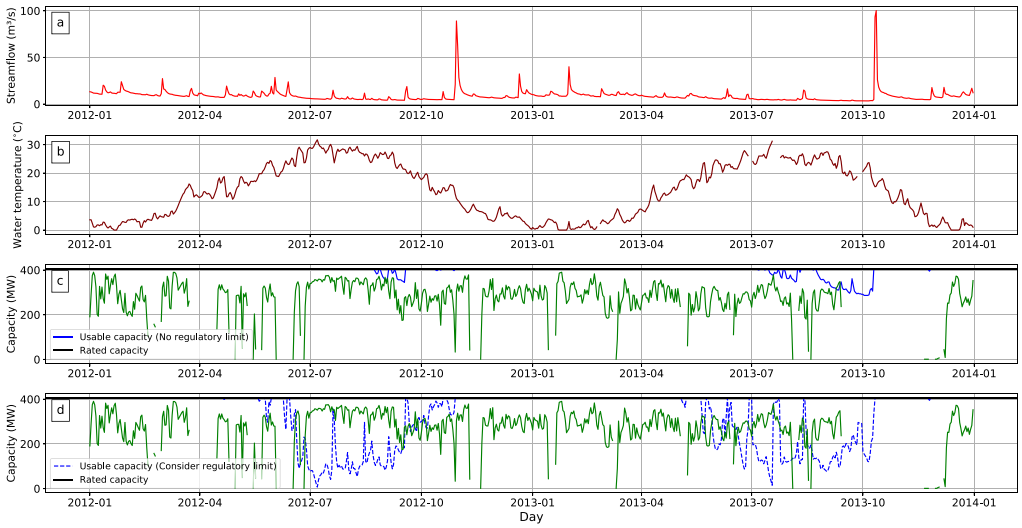

Fig. 3. Calculated daily usable capacity of the Brunner Island plant (unit 2) in Pennsylvania during 2012–2013. a, Historical streamflow available to the power plant. b, Historical water temperature of the intake water. c, Calculated usable capacity without water discharging temperature limit. d, Calculated usable capacity considering regulatory limit.

$$W_{evap,i} = \frac{W_{circ,i} \cdot (n_{cc} - 1)}{\sigma \cdot n_{cc}} (\omega_{out,i} - \omega_{in,i}) \tag{12}$$

$$W_{bd,i} = \frac{W_{circ,i}}{\sigma \cdot n_{cc}} (\omega_{out,i} - \omega_{in,i}) \tag{13}$$

Combining Eqs. (8) and (9) with Eq. (7), an expression for the condenser load can be developed:

$$\begin{aligned} H_{load,i} = & \frac{\rho_w \cdot W_{circ,i}}{\sigma} [h_{a,out,i} + T_{c,i} \cdot c_{p,w} \cdot (\omega_{out,i} - \omega_{in,i})/n_{cc} \\ & - T_{mu,i} \cdot c_{p,w} \cdot (\omega_{out,i} \\ & - \omega_{in,i}) - h_{a,in,i}] \end{aligned} \tag{14}$$

According to heat balance and mass balance equations, the usable capacity of thermoelectric power plant with recirculating cooling can be calculated using Eq. (15).

$$\begin{aligned} P_{rc,i} = & \rho_w \cdot W_{circ,i} \cdot [h_{a,out,i} + T_{c,i} \cdot c_{p,w} \cdot (\omega_{out,i} - \omega_{in,i})/n_{cc} \\ & - T_{mu,i} \cdot c_{p,w} \cdot (\omega_{out,i} - \omega_{in,i}) \\ & - h_{a,in,i}]/(\sigma \cdot \frac{1 - \eta_{net,i} - k_{os,i}}{\eta_{net,i}}) \end{aligned} \tag{15}$$

The relationship between W_{circ} and W_{mu} is given in Eq. (16).

$$W_{circ,i} = \min(W_{mu,i}, \gamma \cdot Q_i) \frac{\sigma}{(\omega_{out,i} - \omega_{in,i})} \tag{16}$$

where Q_i is the real-time streamflow of the river from which the plant withdraws cooling water (m^3/s). W_{mu} can be calculated using Eq. (17).

$$W_{mu,i} = \frac{n_{cc}}{n_{cc} - 1} \frac{P_{n,i} \cdot \frac{(1 - \eta_{net,i} - k_{os,i})}{\eta_{net,i}} \cdot (1 - k_{sens,i})}{\rho_w \cdot h_{fg}} \tag{17}$$

Atmospheric parameters in Eq. (15) are derived from atmospheric parameters (including dry-bulb air temperature T_d, total ambient pressure p_{tot}, and relative humidity RH) using the following equations:

$$\begin{aligned} \omega_{in,i} &= \frac{B \cdot p_{w,i}}{p_{tot,i} - p_{w,i}} \\ \omega_{out,i} &= \frac{B \cdot p_{ws,i}}{p_{tot,i} - p_{ws,i}} \\ h_{a,in,i} &= T_{d,i} \cdot (1.01 + 0.00189\omega_{in,i}) + 2.5\omega_{in,i} \\ h_{a,out,i} &= T_{d,i} \cdot (1.01 + 0.00189\omega_{out,i}) + 2.5\omega_{out,i} \\ T_{c,i} &= T_{wb,i} + T_{app,i} \end{aligned} \tag{18}$$

where B is a constant value and $B = 621.9907 g/kg$. K is the psychrometer constant and $K = 0.000662\ °C^{-1}$. Typically, T_{app} ranges between 4 to 8 °C. T_{wb} is the wet-bulb temperature, and it can be calculated using Eq. (19) if it is unknown.

$$T_{wb,i} = T_{d,i} - \frac{p_{ws,i} - p_{w,i}}{K \cdot p_{tot,i}} \tag{19}$$

In Eq. (19), p_w is the vapor pressure which can be calculated using relative humidity (RH) and saturated vapor pressure (p_{ws}):

$$\begin{aligned} p_{w,i} &= \frac{p_{ws,i} \cdot RH_i}{100} \\ p_{ws,i} &= A \cdot 10^{(\frac{m \cdot T_{d,i}}{T_{d,i} + T_n})} \end{aligned} \tag{20}$$

where A, m, T_n are constants provided in [43].

To calculate daily usable capacity of units with RC cooling systems using Eq. (15), the following steps are required:

(1) Identify all the at-risk RC cooling thermoelectric generators in the PJM and SERC regions.
(2) Obtain the plant-level hydrological and meteorological conditions for each identified at-risk plant.
(3) Calculate the daily usable capacity of each at-risk plant using Eq. (15).

The process to calculate the usable capacity of RC cooling thermoelectric power plants is presented in Algorithm 3.

To identify at-risk RC cooling thermoelectric plants in the PJM and SERC regions, a two-step process is followed: (1) Select all steam turbines (including conventional steam turbine, combined cycle steam, and binary cycle) in the PJM and SERC regions that use recirculating cooling. This information can be obtained from Forms EIA-860 (2022 version) and EIA-923. (2) Classify each plant as an at-risk unit if it uses fresh surface water as the water source for its cooling system, while plants that use ocean water, ground water, or other sources are not considered at-risk during drought conditions. The water source information for each plant is given in Form EIA-860 (2022 version). The at-risk RC cooling thermoelectric generators in the PJM and SERC regions have been identified, and the detailed information is available upon request. In total, there will be 380 at-risk RC cooling thermoelectric generators in the study region by the summer of 2025. The historical daily streamflow and water temperature data can be gathered from the USGS water information dataset [37]. If the historical data of specific surface-water sites is missing, historical data and hydrological models can be used to simulate hydrological conditions. Meteorological data (air temperature, relative humidity, etc.) of each at-risk RC cooling thermoelectric generators were gathered from Daymet dataset [44].

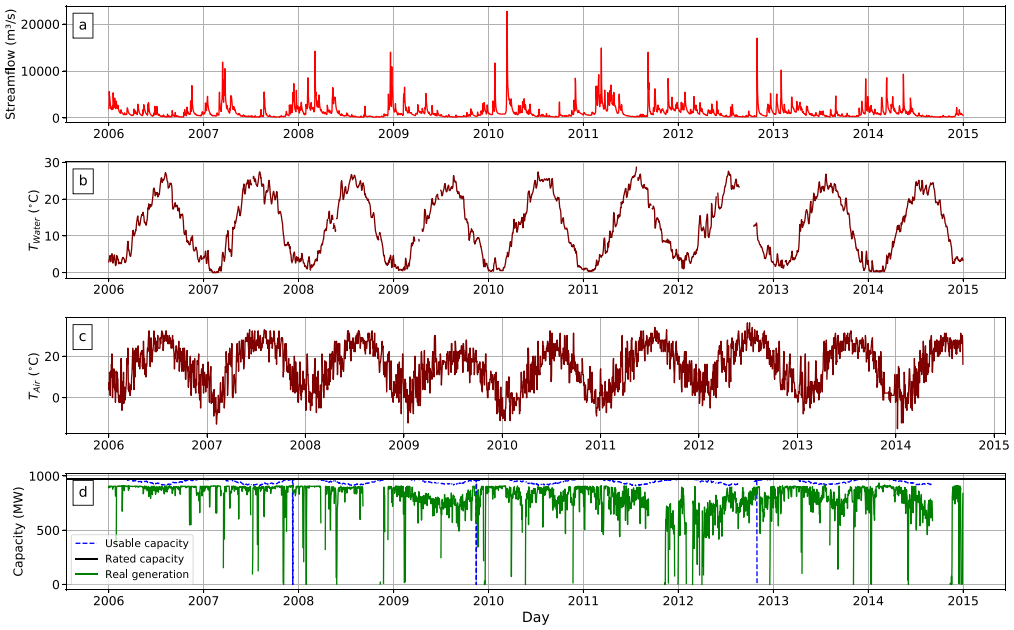

Fig. 4. Calculated daily usable capacity of the Conemaugh plant (unit 1) in PJM during 2006–2014. a, Historical streamflow available to the power plant. b, Historical water temperature of the intake water. c, Historical air temperature of the intake water. d, Calculated daily usable capacity.

Algorithm 3 Generation capacity evaluation algorithm for thermoelectric power plant with recirculating cooling

Input: Thermoelectric power plant information; Streamflow, water temperature, air temperature, humidity, etc.
Output: Available daily generation capability of each thermoelectric power plant with RC cooling.

1: Identify all at-risk RC cooling thermoelectric power plant according to the water source information;
2: **for** Every at-risk power plant with RC cooling **do**
3: Get the location, installed capacity $P_{n,i}$, net efficiency $\eta_{net,i}$ information of the ith RC cooling thermoelectric power plant;
4: **for** Every time step **do**
5: 1) Acquire streamflow Q_i^t value, water temperature $T_{c,i}^t$, air temperature $T_{d,i}^t$, ambient pressure, and relative humidity at the location of the plant;
6: 2) Based on equation (15), calculate the daily usable capacity of the plant;
7: **end for**
8: **end for**

Using the above equations, the daily usable capacity of at-risk recirculating plants in the PJM and SERC regions can be calculated. Fig. 4 illustrates the computed usable capacity of Unit 1 at the Conemaugh plant in the PJM region spanning the years 2006 to 2014. The results indicate that increased air and water temperatures significantly reduced the unit's usable capacity. And the consistent trend of the calculated usable capacity exceeding the unit's actual power output adds credibility to the validity of the capacity derating model.

2.5. Combustion turbine capacity derating

When it comes to the effects of summer drought, the generation of combustion turbines is mainly affected by the dry bulb temperature of the ambient air. The power output of simple-cycle combustion turbines is inversely proportional to the ambient air temperature, with a loss of approximately 0.7–1.0% of capacity for every degree Celsius above 15 [20,45,46]. In this study, the following equation is utilized to model the impact of summer drought on the usable capacity of combustion turbines:

$$P_{ct,i} = \begin{cases} P_{n,i}, & \text{if } T_{d,i} \le 15\ ^\circ\text{C} \\ P_{n,i} \cdot [1 - c_{ct} \cdot (T_{d,i} - 15)], & \text{otherwise} \end{cases} \tag{21}$$

where c_{ct} represents the power-temperature coefficient (0.0083/°C in this study).

In this study, at-risk combustion turbines in the PJM and SERC regions were selected based on generation technology information provided by Form EIA-860 (2022 version). Generator location information at the load zone level was used to obtain meteorological parameter (i.e., dry bulb air temperature), to calculate usable capacity. In total, there will be 2,761 combustion turbines in the study region by the summer of 2025. The process to calculate the usable capacity of combustion turbines is presented in Algorithm 4.

Algorithm 4 Generation capacity evaluation algorithm for combustion turbines

Input: Combustion turbine information; Air temperature.
Output: Generation capability of each combustion turbine.

1: **for** Every combustion turbine **do**
2: Get the location, installed capacity $P_{n,i}$ information of the ith combustion turbine;
3: **for** Every time step **do**
4: 1) Acquire air temperature $T_{d,i}^t$ at the location of the plant;
5: 2) Based on equation (21), calculate the usable capacity of the plant;
6: **end for**
7: **end for**

2.6. Solar PV and wind available capacity

The power output of PV panels is determined by solar irradiance and system conversion efficiency (such as PV module efficiency and inverter efficiency). According to the relative PV performance model described by Ref. [47], the power output from a given PV panel is calculated from the in-plane irradiance I and module temperature T_{mod}:

$$P_{pv}(I, T_{mod}) = P_{STC} \cdot \frac{I}{I_{STC}} \cdot \eta(\hat{I}, \hat{T}) \tag{22}$$

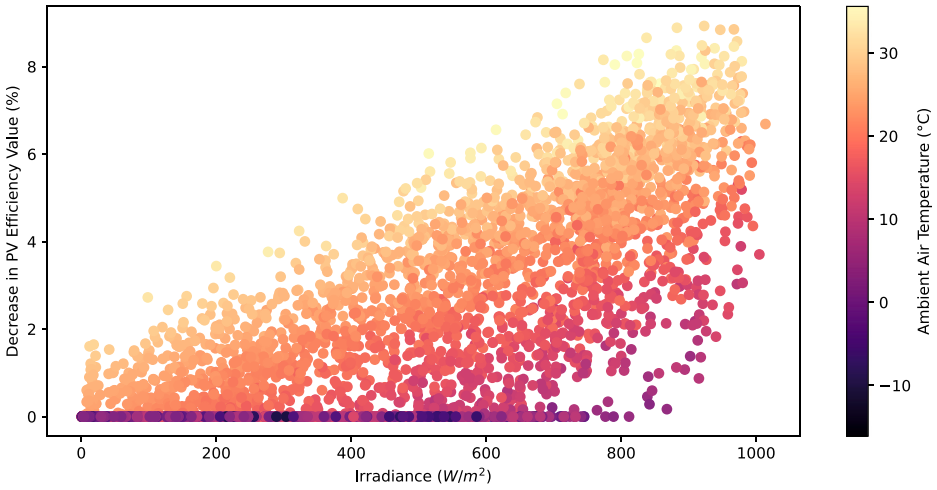

Fig. 5. Visualizing the influence of air temperature and irradiance on PV generation efficiency.

where P_{STC} is the power at standard test conditions (STC) of I_{STC} = 1000 W/m^2 and T_{mod_STC} = 25 °C. $\eta(\cdot)$ is the instantaneous relative efficiency coefficient, which is affected by in-plane irradiance and module temperature, as illustrated in Fig. 5. In the equation, $\hat{I}$ and $\hat{T}$ are normalized parameters to STC values $\hat{I} \equiv I/I_{STC}$ and $\hat{T} \equiv T_{mod} - T_{mod\_STC}$. T_{mod} can be determined from the ambient air temperature T_d. According to [48], during steady-state or slowly changing conditions, the module temperature can be approximated by the sum of the ambient temperature and a coefficient c_T multiplied by the irradiance:

$$T_{mod} = T_d + c_T \cdot I \tag{23}$$

Typically, the coefficient c_T falls within the range of 0.025 to 0.05 °C W^{-1} m^2. To simplify the model in Eq. (22), the cell temperature coefficient is usually utilized to estimate changes in efficiency (η), where the coefficient usually varies from −0.5%/°C to −0.2%/°C [49]. This implies that for every degree increase in module temperature above 25 °C, the efficiency of the panel decreases by 0.2% to 0.5%.

In this study, the above model is utilized to compute the hourly power output of solar PV plants in the PJM and SERC regions under summer drought conditions. The location and installed capacity details of all 1880 solar PV generators in the study region as of the summer of 2025 were collected from Form EIA-860 (2022 version). Historical weather data, including solar irradiance and air temperature, were retrieved from NASA's MERRA-2 dataset [50]. The Global Solar Energy Estimator (GSEE) package [48] was employed to calculate the generation curve for all solar PV generators. The process to calculate the usable capacity of solar PV generators is presented in Algorithm 5.

Algorithm 5 Generation capacity evaluation algorithm for solar PV

Input: Solar PV plants information; Irradiation and air temperature information.

Output: Generation capability of each solar PV plant.

for Every solar PV plant **do**
  Get the location, installed capacity $P_{n,i}$ information of the ith solar PV plant;
  for Every time step **do**
    1) Acquire irradiation I_i and air temperature $T_{d,i}$ at the location of the plant;
    2) Based on equation (22), the generation capacity of the solar PV plant is calculated using the GSEE;
  end for
end for

The available capacity of wind power generators is contingent upon the wind speed. Fig. 6 shows the power output curves of various types of wind turbines. When the wind speed falls below the turbine's cut-in speed or exceeds the cut-out speed, the power output remains at zero. It is worth noting that each type of wind turbine exhibits distinct power-wind speed characteristics. To determine the daily wind generation of each wind generator in the PJM and SERC regions, the location and installed capacity data for all wind generators were collected from Form EIA-860 (2022 version). By the summer of 2025, there will be a total of 148 wind generators in the study region. The generation of wind generators is computed using the Virtual Wind Farm (VWF) model [51], which calculates generation based on the wind speed and the power output characteristics of the wind turbine as illustrated in Fig. 6. The process of evaluating wind fleet generation capability is given in Algorithm 6.

Algorithm 6 Wind turbine generation capacity evaluation algorithm

Input: Wind turbine information; Wind speed.

Output: Generation capability of each wind turbine.

for Every wind turbine **do**
  Get the location, hub height, wind turbine type information of the ith wind turbine.
  for Every time step **do**
    1) Obtain wind speeds at 2, 10, and 50 meters above ground, corresponding to the wind turbine's location.
    2) Extrapolates speeds to the hub height of the turbine.
    3) Utilizing the manufacturer's power curves (as depicted in Fig. 6), which are specific to the wind turbine, convert wind speeds to power output.
  end for
end for

3. Simulation results

In this section, the developed capacity derating framework is applied to a real-world case study, evaluating the usable generating capacity of the 2025 power generation fleet within the EI during past summer drought conditions. Details on the generation fleet and the impacts of extreme drought conditions are presented.

3.1. Generation fleet of Eastern Interconnection

Historically, summer droughts have predominantly affected the southeastern portion of EI's service territory. For instance, a notable drought occurred in the Southeast region during 2007–2008, as illustrated in Fig. 7. This particular drought event stands out as the

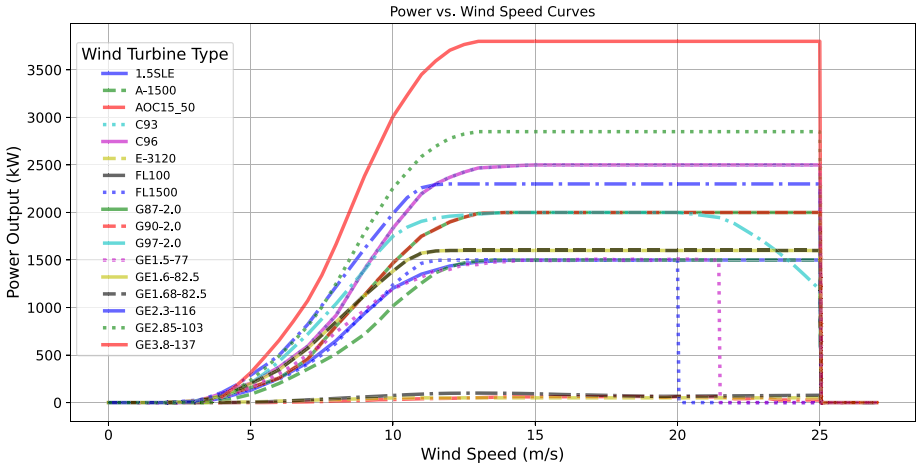

Fig. 6. Power output curves of different wind turbines.

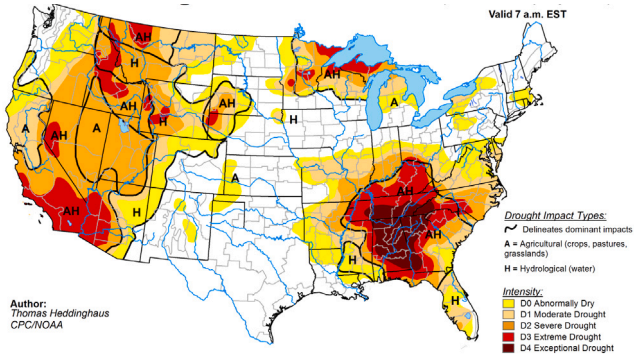

Fig. 7. Drought map of United States on August 28, 2007 [52].

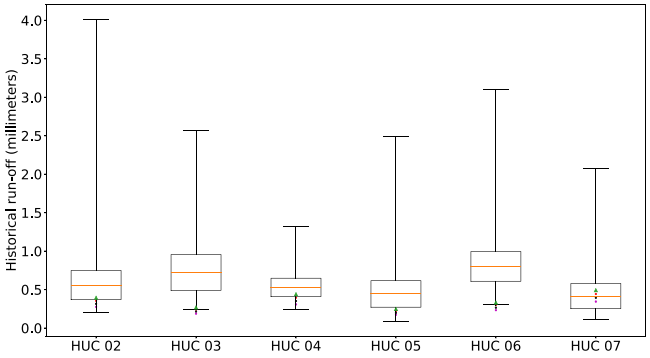

Fig. 8. The past 100 years summer run-off distribution for hydrologic unit code (HUC) 02 to HUC 07 regions. The PJM and SERC encompass 6 HUC regions (HUC 02 to HUC 07) in the southeastern United States. The green triangle point represents run-off in the summer of 2007. The red, black, and magenta points represent decreasing rainfall by 10%, 20%, and 30%, based on values from the summer of 2007, respectively.

second driest on record for the region, with exceptionally low rainfall across many states (e.g., Alabama, North Carolina, Tennessee, etc.), visually depicted in Fig. 8. Consequently, this study primarily focuses on evaluating the impact of summer droughts on the SERC region, containing this drought-prone Southeastern region, as well as the PJM region. SERC is responsible for ensuring a reliable and secure electric grid across the southeastern and central states, mainly including Kentucky, Tennessee, North Carolina, Alabama, Georgia, and South Carolina. PJM, or the PJM Interconnection LLC, is a regional transmission organization in the United States, serving all or parts of Delaware, Illinois, Indiana, Kentucky, Maryland, Michigan, New Jersey, North Carolina, Ohio, Pennsylvania, Tennessee, Virginia, West Virginia, and the District of Columbia.

The proposed available generation capacity assessment framework was applied to the real-world generation fleet in the PJM and SERC regions, which at present provides over 400 GW of generating capacity. The real-world generation fleet of the region was ascertained using Form EIA-860, and comprises over 3,000 thermal, 773 hydro, and numerous other power plants (e.g., solar PV, wind turbines, etc.). In 2025, 83% of the installed capacity will be contributed by thermal (including coal, nuclear, and natural gas, etc.), while the penetration of renewable energy (e.g., hydro, solar PV, and wind) will remain relatively low, constituting only 16.1%. Compared to the fleet at large, 94.9% of conventional steam coal plants, 88.2% of natural gas fired combined cycle, and 89.2% of nuclear plants will likely be affected by summer drought events. Table 1 summarizes the overall installed capacity of the study region, as well as the at-risk capacity by generating technology. The locations of the at-risk thermal and hydro plants are illustrated in Fig. 9. In general, most of these at-risk generators are in close proximity to rivers. All combustion turbines and renewable energy generators are also considered at-risk units. Information regarding various power plants, encompassing details like their names, installed capacities, locations, primary generation technologies, cooling systems, and water sources and discharge points, was sourced from the EIA-860 [39] and EIA-923 [40]. Hydrological data, including streamflow and water temperature, were obtained from the USGS water information dataset [37]. Meteorological data, such as air temperature, relative humidity, wind speed, and solar irradiance, were gathered from the Daymet dataset [44] and NASA's MERRA-2 dataset [50].

3.2. Available capacity distributions of individual generation units under historical summer conditions

The daily usable capacity of any generator, as depicted in Fig. 9, can be computed utilizing the plant-level capacity derating models presented previously in Section 2. Analyzing the available capacity of different generating technologies during summer weather conditions from 2006 to 2019 revealed substantial impacts on at-risk conventional generators. There are notable differences in the capacity distribution among various generating technologies, as illustrated in Fig. 10. The daily usable capacity patterns of the three hydro units (see Fig. 10(b)) exhibit similarities, with their daily usable capacity frequently falling below 40% during most summer periods due to limited streamflow conditions. In contrast, the daily usable capacity distributions of the three ON units widely differ from each other (see Fig. 10(c)). For

Table 1
Installed generation capacity in the PJM and SERC regions by 2025.

Category	Installed capacity (MW)	Percent of total capacity	At-risk capacity (MW)	Percent of category
Conventional steam coal	83,634.5	20.1%	79,335.9	94.9%
Natural gas fired combined cycle	110,043.7	26.4%	97,060.6	88.2%
Combustion turbine	71,311.8	17.1%	71,311.8	100%
Nuclear	63,567.1	15.3%	56,727.8	89.2%
Natural gas steam turbine	12,301.3	3.0%	8664.9	70.4%
Conventional hydro and PHS	26,089.2	6.3%	14,762.6	56.6%
Solar PV	28,313.4	6.8%	28,313.4	100%
Wind	12,536.7	3.0%	12,536.7	100%
Wood/Wood waste biomass	3855.6	0.9%	2453.1	63.6%
Other	4713.8	1.1%	443.7	9.4%
Total	**416,367.1**	**100%**	**371,610.5**	**89.3%**

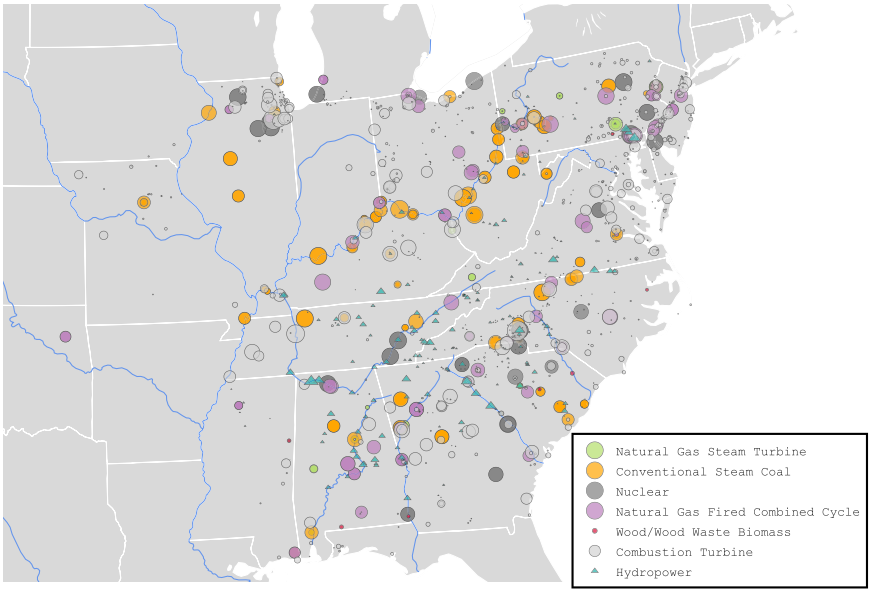

Fig. 9. Locations of at-risk conventional power plants in the PJM and SERC regions. The white line indicates the state boarder. The blue line indicates the river in the region.

example, the ON@1 unit, a nuclear power plant located in Tennessee, shows minimal impact on its capacity from historical summer weather. This resilience can be attributed to the availability of sufficient cooling water from the Tennessee River, meeting the plant's needs during the historical summer periods. On the contrary, the other two ON units show significant impacts from summer weather. The daily usable capacity patterns of the three RC units (see Fig. 10(d)) exhibit similarities, with their daily usable capacity being less affected by summer weather conditions compared to hydro and ON units. The daily usable capacity patterns of the three CT units (see Fig. 10(e)) also display similarities. The limited impact of summer weather conditions on RC and CT units is attributed to the fact that these two generating technologies are primarily influenced by meteorological conditions, implying that decreased streamflow rates have less impact on their capacities.

To gain a deeper understanding of how summer weather affects the available capacity of individual generators, the average usable capacity for each at-risk unit is computed during the summer season. The summer season average usable capacity of the ith at-risk unit is defined as:

$$CF_i^{avg} = \frac{1}{T}\sum_{t=1}^{T}\frac{P_i^t}{P_{n,i}} \tag{24}$$

Here, T denotes the time span of the summer season. In this study, a total of 773 hydro units, 137 ON units, 380 RC units, and 2,761 CT units were analyzed. Fig. 11 depicts the histograms representing the summer average available capacity distribution of at-risk units in the study region. The summer average usable capacity of hydro units exhibits a relatively even distribution between 0 and the rated capacity, and 10.2% of hydro units remain unaffected throughout the summer conditions (see Fig. 11(a)). For the subset of at-risk thermal units equipped with ON cooling, 35% of ON units consistently evade impacts under historical summer conditions from 2006 to 2019. The average usable capacity of the remaining ON units fluctuates between 0 and the rated capacity, as depicted in Fig. 11(b). Fig. 11(c) reveals that the average usable capacity of 95.5% of RC units surpasses 90% of their rated capacity. Concerning CT units, their average usable capacity under historical summer conditions ranges from 94% to 97% of the rated capacity, as shown in Fig. 11(d). The findings depicted in Fig. 11 align with those in Fig. 10, reinforcing the observation that RC and CT units demonstrate greater resilience compared to hydro and ON units.

3.3. Available capacity of generation fleet under historical summer conditions

After obtaining the daily available capacity of each at-risk unit, the effects of summer drought on the capacity of the generation fleet can be explored. The available capacity of each generation category is defined as:

$$CF_g^t = \frac{\sum_{i\in g} P_i^t}{\sum_{i\in g} P_{n,i}} \tag{25}$$

where, CF_g^t denotes the available capacity percentage of category g at time t, and $g \in \{Hydro, ON, RC, CT, PV, WT\}$.

Based on the meteorological and hydrological conditions in the study region from 2006 to 2019, the summer available capacities of the

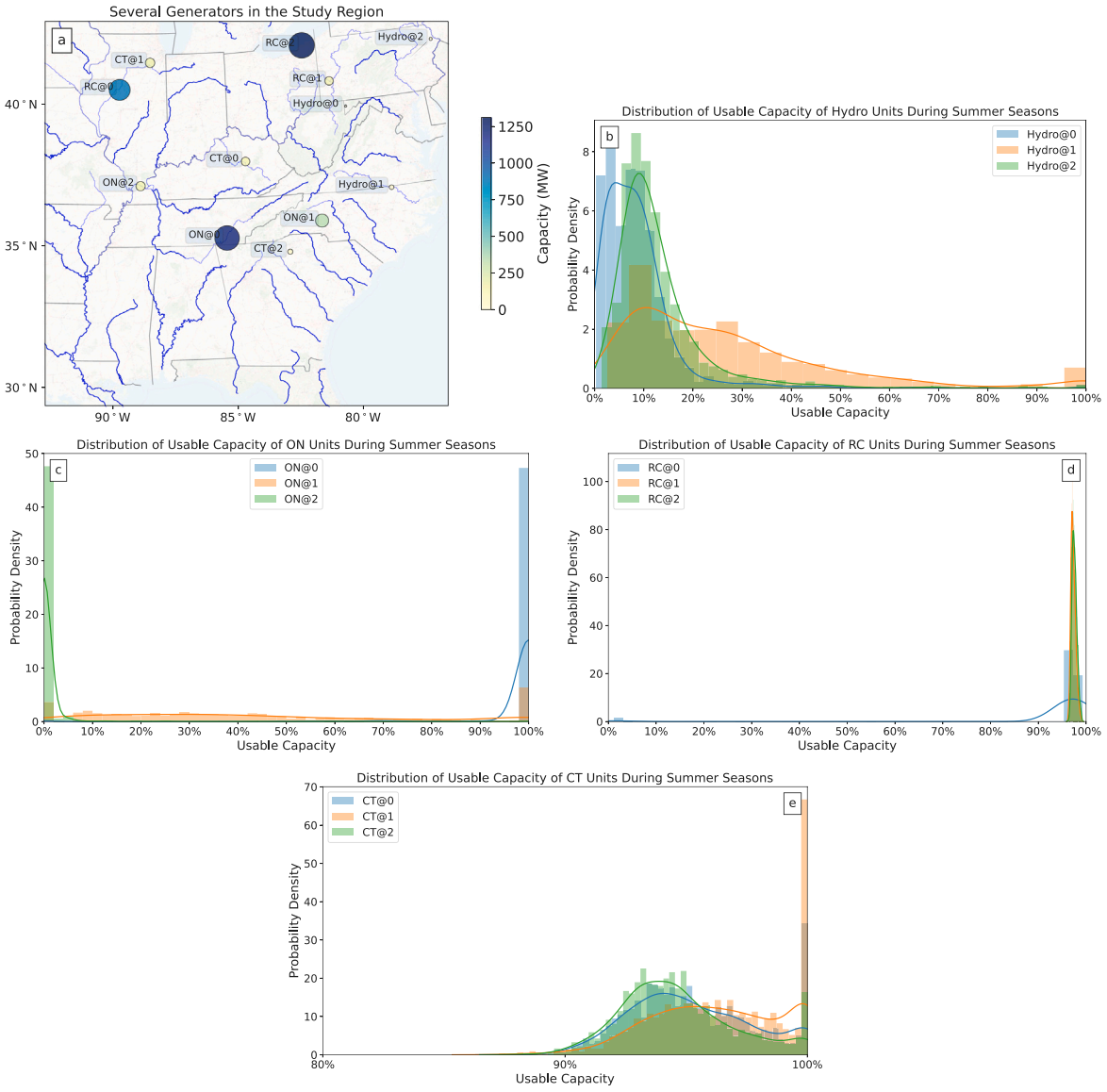

Fig. 10. Daily usable capacity distribution of several selected units during the summer seasons from 2006 to 2019. a, Location of the generation units. The blue lines in the figure represent the rivers in the region. b, Usable capacity distribution of the three hydro units (i.e., Hydro@1, Hydro@2, and Hydro@3). c, Usable capacity distribution of the three ON units (i.e., ON@1, ON@2, and ON@3). d, Usable capacity distribution of the three RC units (i.e., RC@1, RC@2, and RC@3). e, Usable capacity distribution of the three CT units (i.e., CT@1, CT@2, and CT@3).

hydro fleet, thermal fleet, and renewable generation fleet were calculated. Fig. 12 illustrates the total available capacity of each generation category. These results yield several valuable insights:

- **The available capacities of the hydro fleet and thermal fleet with ON cooling systems could be significantly affected by hydrological conditions.** Fig. 12(a) reveals that, during the summer seasons, the total daily usable capacity of all conventional hydro power plants in the region varies between 10% and 70%. In a normal summer, such as that of 2015, the median value of the daily usable capacity of the hydro fleet during the season typically falls between 30% and 40% of the total installed capacity. During a wet summer, such as 2018, the median daily usable capacity of the hydro fleet can surpass 50% of the total installed capacity, reaching peaks of 70%. In contrast, during a drought summer, such as 2007, the median daily usable capacity of the hydro fleet can dropped to around 20% of the total installed capacity, reaching low values of around 15%. For thermal power plants with once-through cooling systems, their total daily usable capacity falls between 45% and 85% during the summer seasons, as shown in Fig. 12(b). In a normal summer, such as that of 2015, the median daily usable capacity of the ON cooling thermal fleet was typically around 65% of the total installed capacity. In a wet summer, the value could approach 70%. Nevertheless, in a drought summer like 2007, the median daily usable capacity of the fleet can decline to approximately 58%, even reaching low values of about 45%. It was also observed that the available capacity range of the ON cooling thermal fleet was relatively narrow compared to the hydro fleet. The primary reasons for the reduced available capacity of the ON cooling thermal fleet are the limited availability of cooling water and an increase in cooling water temperature.
- **The impact of hydrological and meteorological conditions on combustion turbines and thermal power plants with RC cooling is relatively minimal compared to hydro and ON cooling based thermal power plants.** In the summer seasons, the total daily usable capacity of all RC cooling based thermal power plants in the region hovers between 80% and 97%, as

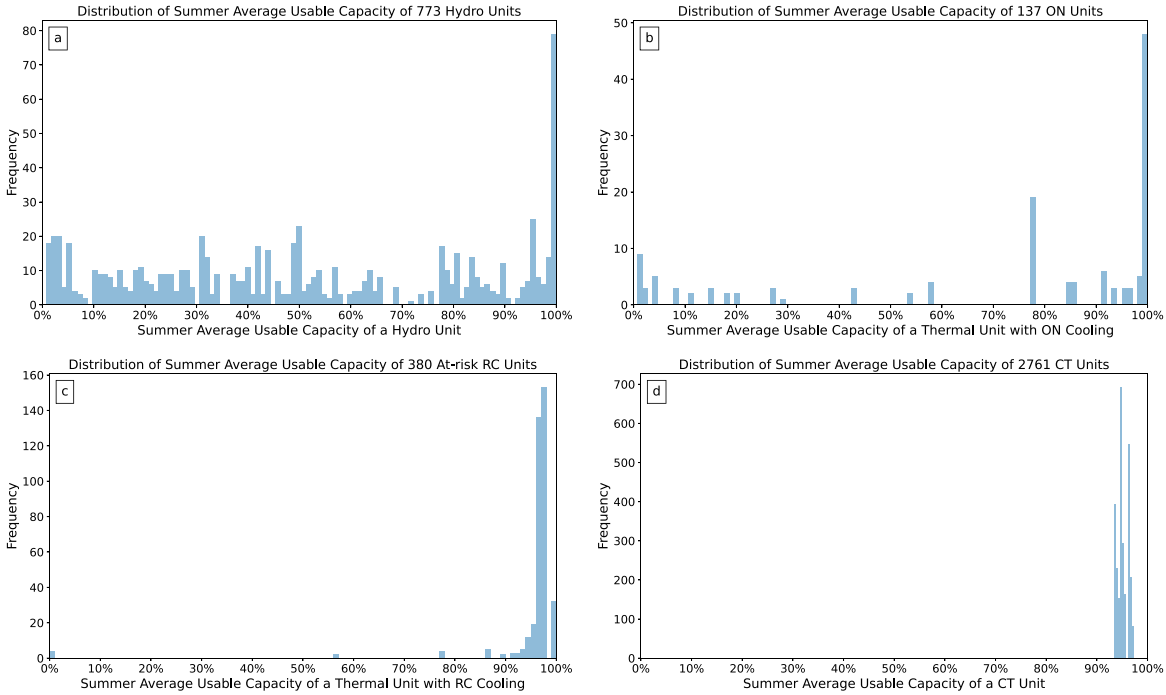

Fig. 11. Summer average usable capacity distribution of at-risk hydro and thermal generators under summer weather from 2006 to 2019. a, Hydro generators. b, At-risk thermal generators with ON cooling. c, At-risk thermal generators with RC cooling. d, At-risk combustion turbines.

depicted in Fig. 12(c). In a normal summer, the median daily usable capacity of the RC cooling-based thermal fleet was typically around 93% of the total installed capacity. Combustion turbines maintain a total daily usable capacity between 90% and 100%, as shown in Fig. 12(d). In a normal summer, the median daily usable capacity of the CT fleet was typically around 95% of the total installed capacity. It can be found that the CT fleet exhibited the lowest summer capacity deration compared to ON and RC cooling-based thermal fleets. Additionally, the range of the total daily usable capacity of both the RC cooling-based fleet and CT fleet was smaller than the ON cooling-based fleet and hydro fleet.

- **The daily available capacity of the solar PV and wind turbine based renewable generation fleet shows no significant differences under historical summer weather conditions.** As shown in Fig. 12(e)–(f), the median daily usable capacity of the solar PV fleet and wind turbine fleet in the region is approximately 23.6% and 21.6% of the total installed capacity, respectively. Compared to normal summers (e.g., 2018), the available capacity of the renewable energy fleet was minimally affected by drought weather conditions in the historical drought summers (e.g., 2007). This can be attributed to the fact that the available solar and wind resources during the summers of 2006–2019 did not exhibit significant differences, as demonstrated in Fig. 13. While the solar PV and wind turbine based renewable energy fleets show greater resilience compared to other power generation methods like hydro and thermal in the PJM and SERC regions during the historical summer conditions, it is crucial to further study how climate-induced extreme summer weather might affect their capacity in future. This is especially important due to the impact of climate change and the rapid growth of renewable energy in power systems. For instance, in 2021, much of Europe experienced a wind drought, where wind speeds dropped by around 10% below the yearly average during the transition from summer to fall [53].
- **The median capacity deration of the at-risk generation fleet under historical summer conditions averages approximately 20.5% of the installed capacity.** For the at-risk thermal fleet in the region, the daily usable capacity ranges from 79% to 95% of the total installed capacity, with the median value hovering around 88%, as depicted in Fig. 14. By integrating the information presented in Fig. 12(a)–(d), it becomes evident that the daily usable capacity of the at-risk generation fleet falls within the range of 71% to 87%, as indicated in Fig. 15. And the median available capacity of the at-risk generation fleet is around 79.5%. The results lead to the observation that the capacity deration of the generation fleet in the region is primarily contributed by the capacity deration of the hydro fleet, PV and wind based renewable generation fleet, as well as the ON cooling based thermal fleet. However, it is important to note that the installed capacity of the power grid is still predominantly composed of RC cooling based thermal fleet (with a total capacity of approximately 130 GW in 2025) and CT fleet (with a total capacity of around 140 GW in 2025). The capacity deration stemming from these generators cannot be disregarded.

3.4. Available capacity under the 2007 southeastern summer drought conditions

Extreme drought event could significantly reduce the available capacity of the generation fleet in the PJM and SERC regions. An analysis of the 2025 generation fleet under the extreme summer drought conditions of 2007 within these regions reveals the following findings:

Vulnerability of Hydro Fleet: The conventional hydro fleet's performance was notably challenged, exhibiting a median usable capacity of just 20% of its installed capacity during this extreme period. This represented a further decrease of 10% to 20% in usable capacity compared to a typical summer, relative to installed capacity. The at-risk thermal fleet showcased a relatively more robust performance, maintaining a median usable capacity of 87%, with only a minor decrease of 2% to 3% compared to a typical summer. This divergence in performance underscores the varying impacts of extreme drought on hydro and thermal generation, as shown in Figs. 12(a) and 14.

Severe Impact on ON Cooling Systems: A detailed examination of the thermal fleet revealed further distinctions in their responses to the

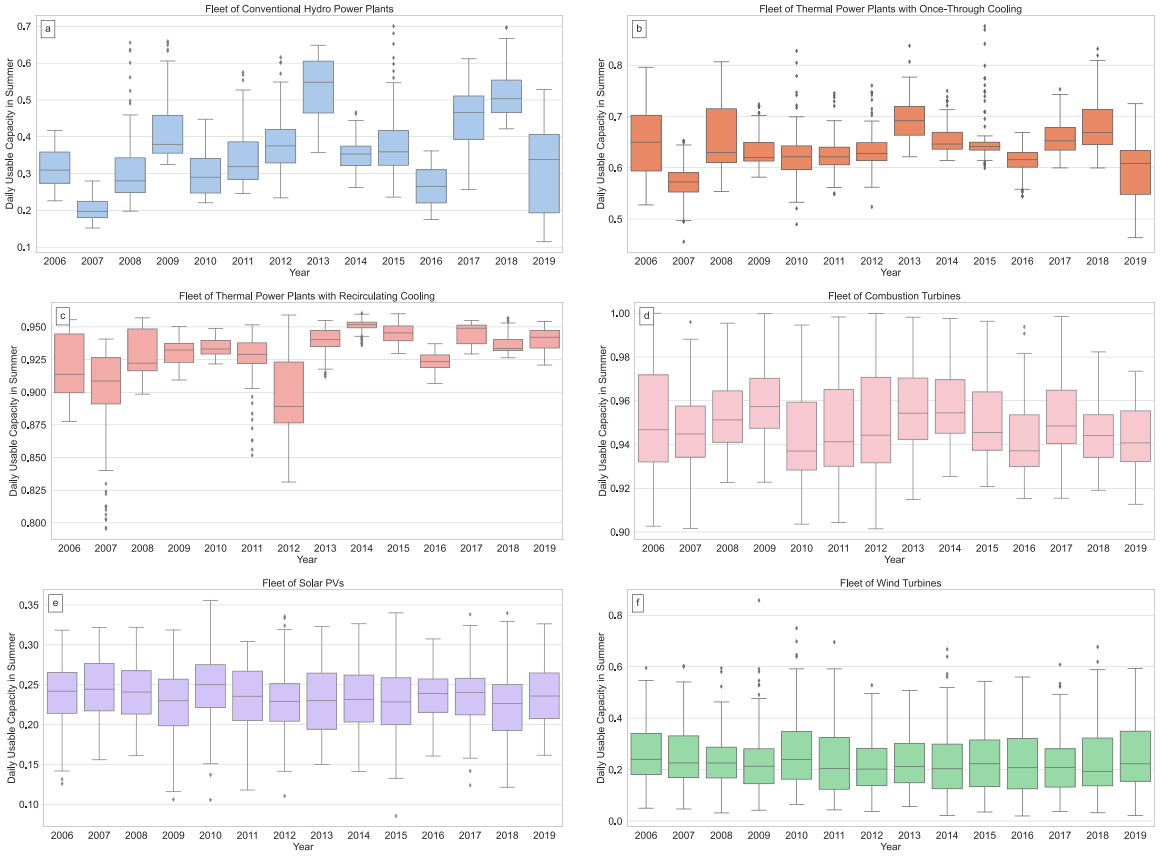

Fig. 12. Total usable capacity of different generation technologies in the 2025 PJM and SERC regions' generation fleet under historical summer conditions from 2006 to 2019. a, Conventional hydro power plants. b, Thermal power plants with once-through cooling. c, Thermal power plants with recirculating cooling. d, Combustion turbines. e, Solar PVs. f, Wind turbines.

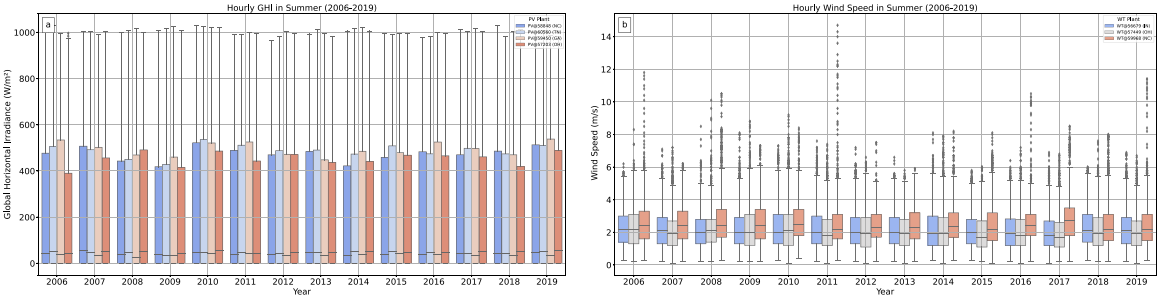

Fig. 13. Hourly solar irradiance and wind speed distributions at selected locations under summer conditions (2006–2019). a, Hourly solar irradiance distribution at four PV plant locations in summer, with installed capacities of 65 MW for PV@58848 (NC), 53 MW for PV@60560 (TN), 80 MW for PV@59450 (GA), and 10 MW for PV@57203 (OH). b, Hourly wind speed distribution at three WT plant locations in summer, with installed capacities of 130.5 MW for WT@56679 (IN), 302 MW for WT@57449 (OH), and 208 MW for WT@59968 (NC).

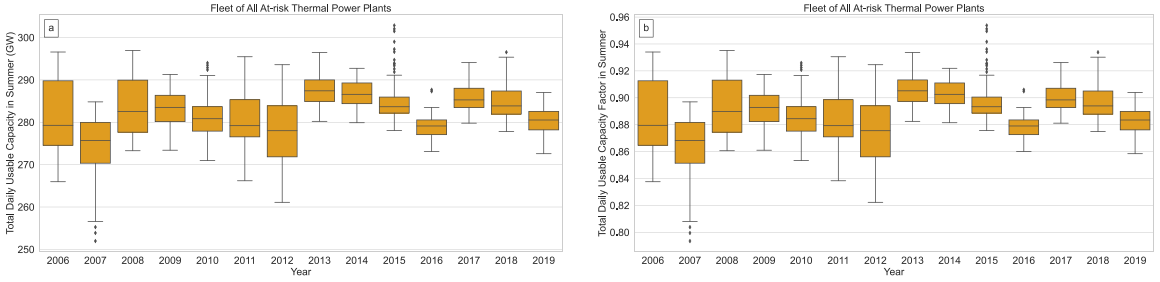

Fig. 14. Total daily usable capacity of all at-risk thermal power plants during the summer season, affected by historical weather conditions from 2006 to 2019, impacting the 2025 generation fleet of the PJM and SERC regions. a, Total daily usable capacity. b, Total daily usable capacity factor.

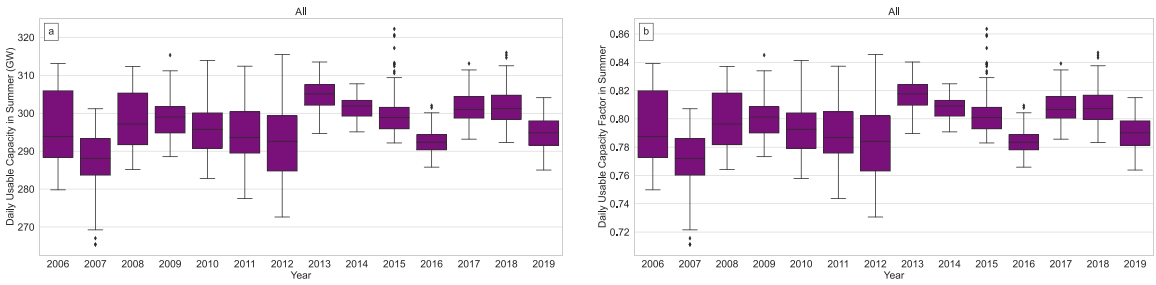

Fig. 15. Total daily usable capacity of at-risk fleet (including all at-risk power plants) during the summer season, affected by historical weather conditions from 2006 to 2019, impacting the 2025 generation fleet of the PJM and SERC regions. a, Total daily usable capacity. b, Total daily usable capacity factor.

2007 extreme drought conditions. A noteworthy observation was thermal power plants utilizing ON cooling systems are highly vulnerable to such drought conditions, experiencing a significant median capacity reduction of 43% (see Fig. 12(b)). This represented a further decrease of approximately 6.3% in usable capacity compared to a typical summer, relative to installed capacity. Given that the total installed capacity of the thermal fleet with ON cooling systems was projected to be approximately 54 GW in 2025, this equated to a substantial reduction of 3.31 GW in available capacity. This vulnerability stemmed from their reliance on open cycle water-dependent cooling systems, where the simultaneous reduction in available water flow and the escalation of water temperatures resulted in a substantial derating of their usable capacity. In contrast, the thermal fleet relying on RC cooling systems exhibited a more moderate median capacity reduction of 9.2%, while combustion turbines showed a median capacity decrease of 5.5% (see Fig. 12(c)–(d)). Combustion turbines and thermal power plants with RC cooling systems were primarily affected by meteorological conditions, resulting in a relatively smaller impact.

Minimal Impact on Available Capacity of Solar PV and Wind, Yet Greater Fluctuations: The solar PV and wind turbine fleets in the region displayed considerable resilience under the 2007 drought conditions. Both maintained median daily usable capacities of approximately 24% and 22.5% of their respective installed capacities, highlighting their ability to withstand extreme drought conditions. While the available capacity of solar PV and wind based generation fleets showed minimal discernible impact during the drought condition compared to a typical summer, it is noteworthy that these technologies exhibited significantly greater fluctuations in normal available capacity compared to hydro and thermal generation (see Fig. 16).

Correlations between Capacity Derations of Different Generation Technologies: The capacity derations of the generators in the PJM and SERC regions exhibit correlations since they are influenced by shared meteorological and hydrological conditions. This correlation is evident in the findings presented in Fig. 16. Under the extreme conditions of the 2007 summer, the minimum total usable capacity of ON, RC, and CT fleets could potentially decline to around 45%, 80%, and 90% of their respective installed capacity. The lowest points in the ON, RC, and CT capacity curves in Fig. 16 align temporally, occurring during the same period from 8/1/2007 to 8/15/2007. This synchronization underscores the shared influence of meteorological and hydrological factors on these generation technologies.

Potential 8.5 GW Reduction in Generation Fleet Capacity during 2007-Style Drought: If conditions similar to the extreme summer drought of 2007 were to recur in the near future, the generation fleet could face a significant decrease of approximately 8.5 GW in available capacity (median value) compared to a typical summer (see Fig. 15(a)). Of this 8.5 GW reduction, the ON fleet would account for 3.31 GW, the RC fleet for 2.60 GW, the CT fleet for 0.20 GW, and the Hydro fleet for 2.35 GW. This scenario would lead to a substantial reduction in the available capacity of the at-risk generation fleet, encompassing all at-risk generators, under the 2007 drought conditions. Usable capacity would range from 71% to 81% of the total installed capacity, as depicted in Fig. 15(b). An in-depth analysis of Fig. 15(a)–(b) further revealed that the total usable capacity of the at-risk fleet reached its nadir under the condition of 2007 summer. This aligns with the fact that the summer of 2007 marked the most severe drought experienced in the region over the past two decades.

The alarming capacity deration can be directly attributed to the severe drought that gripped the region. Fig. 17(a) reveals the grim reality of the 2007 summer, showcasing that the average daily maximum temperature in numerous states within the SERC region soared above 34 °C. Even certain areas within the PJM region experienced average temperatures exceeding 30 °C. This scorching heatwave added an additional layer of complexity to the power generation challenge. Figs. 17(b) and 8 underscore the historic nature of the drought's impact, with both figures indicating record-low precipitation levels in the region. This scarcity of rainfall, in combination with the sweltering heat, resulted in a critical reduction in available water flow, making it exceedingly difficult for water-dependent power generations.

3.5. Sensitivity of available capacity to temperature and streamflow

In the face of the escalating impact of climate change, a troubling trend of increasingly severe extreme drought events has emerged. In response to this evolving landscape, an analysis was conducted to assess the sensitivity of the available capacity of the 2025 generation fleet within the PJM and SERC regions to variations in air temperature and streamflow. To establish a reference point, the 2007 summer drought was employed as the baseline scenario. Subsequently, the study explored the effects on the usable capacity of hydro and thermal power plants under six additional scenarios. In the first set of scenarios (C1, C2, and C3), the study examined the consequences of increasing air temperatures by 1 °C, 2 °C, and 3 °C, respectively, while maintaining remaining meteorological conditions consistent with those observed during the 2007 summer. The impact of increased air temperature on hydrological conditions (such as water temperature) was modeled using the Soil & Water Assessment Tool (SWAT) [54]. In the second set of scenarios (R10, R20, and R30), the study investigated the effects of decreasing streamflow by 10%, 20%, and 30%, respectively, while maintaining consistent meteorological conditions similar to those of the 2007 summer. The influence of reduced streamflow on hydrological conditions was also modeled using SWAT.

The outcomes of the analysis are presented in Fig. 18. Fig. 18(a) illustrates that with every 10% reduction in streamflow compared to the 2007 summer drought conditions, the median daily available capacity of the hydro fleet decreased by 1.40%. In Fig. 18(b), it can be observed that for every 1 °C increase in air temperature from the 2007 summer drought conditions, the median daily available capacity of the thermal fleet decreased by 0.60%. Furthermore, each 10% reduction in streamflow from the 2007 summer drought conditions resulted in a 0.22% decrease in the median daily available capacity of the thermal fleet. These findings underscore the vulnerabilities of power generation in the face of climate change and emphasize the critical necessity for the development of adaptation and mitigation strategies to ensure energy resilience in the near future.

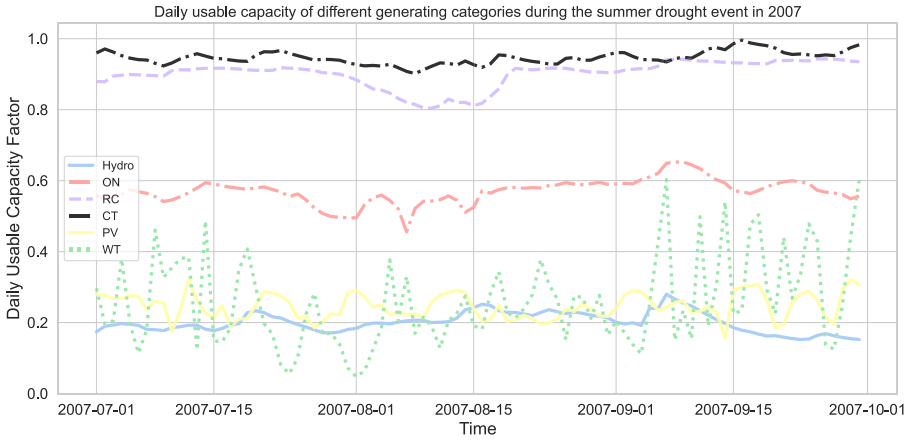

Fig. 16. Calculated daily usable capacity of different generating categories under the 2007 Southeastern summer drought event.

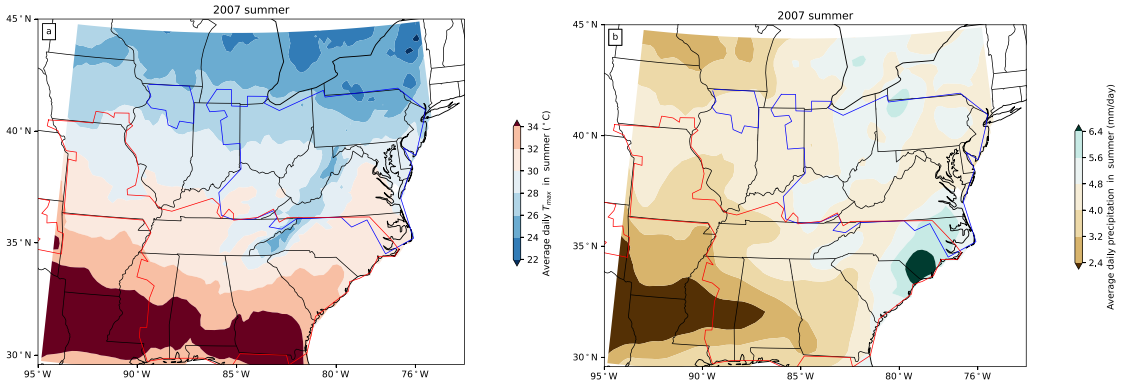

Fig. 17. Weather condition of the PJM and SERC regions during the 2007 Southeastern summer drought event. a, Average daily maximum temperature of the regions. b, Average daily precipitation of the regions. The region indicated by the blue solid line represents the service territory of PJM, while the one marked by the red solid line corresponds to the service territory of SERC.

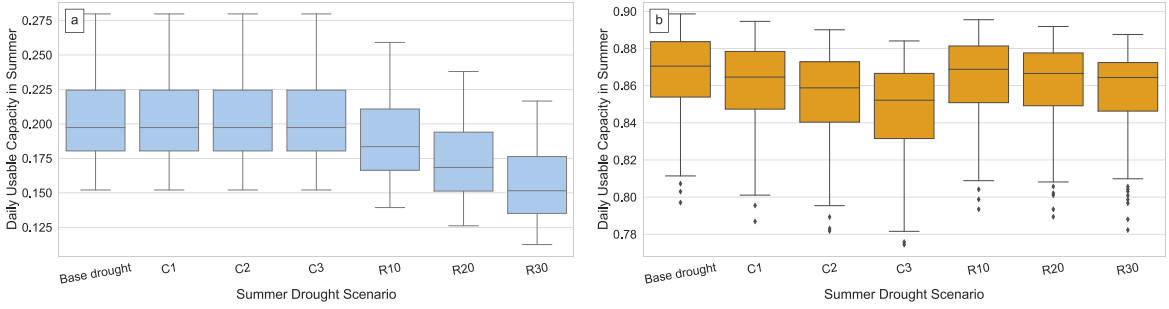

Fig. 18. Daily usable capacity of the generation fleets in the PJM and SERC regions under different summer drought scenarios. a, Hydro generation fleet. b, Thermal generation fleet.

4. Discussion

The proposed framework is distinguished by its systematic and high-resolution evaluation, which assesses the capacity of diverse generating technologies across an extensive geographical region. This methodology effectively tackles the limitations identified in previous research, as discussed in the literature review section. One of its prominent advantages is its ability to facilitate a comprehensive impact assessment of extreme summer drought on hydro, thermal, and VRE fleets at the plant level, incorporating hydrological and meteorological conditions. From a practical perspective, the key strength of this methodology lies in its adaptive capability to accurately evaluate the daily available capacity of generators under unprecedented drought scenarios, which have not been historically observed. It can capture correlations among the weather-dependent available capacities of various generators. While the quantitative results presented in this study are specific to the PJM and SERC regions in the United States, the framework can be readily extended to other regions, such as the Western Interconnection region.

The findings of this study reveal that the available capacity distributions of individual generation units, even those utilizing identical generating technologies, exhibit variation under historical summer conditions. These results underscore the necessity of plant-level modeling for precise assessment of the generating fleet's available capacity. In the PJM and SERC regions, conventional hydro and thermal units are projected to remain the predominant generation resources in the near term. The quantitative analysis provided herein indicates that the available capacity of these conventional generation resources is particularly vulnerable to extreme drought events. Notably, the available capacities

of hydro fleets and thermal fleets equipped with ON cooling systems are significantly influenced by hydrological conditions. In the most severe drought scenario of the past two decades, the usable capacity of the hydro fleet and the ON-based thermal fleet could plummet to as low as approximately 15% and 45% of their respective installed capacities. Given the ongoing use of ON cooling techniques by some aging coal-fired and nuclear power plants within the study region, the derating or potential shutdown of these substantial generators during drought periods could exert a substantial influence on the economic and secure operation of the EI system. One potential measure to enhance the resilience of these thermal power plants during extreme summer drought conditions is the replacement of ON cooling systems with more robust RC cooling systems.

Regarding the hydro fleet, this study reveals that the calculated usable capacity (median value) of the hydro fleet falls within the range of 30% to 55% of the total installed capacity. In comparison, data from a DOE report [55] indicate that the median U.S. hydropower capacity factor between 2005 and 2018 fluctuated between 35% and 45%, highlighting the region's relatively robust hydro resource potential. Considering the potential decline in the hydro fleet's usable capacity to as low as approximately 15% of its installed capacity, it is advisable for stakeholders to pursue collaborative strategies with water resource management authorities. Implementing strategic measures, like enhancing water storage in reservoirs to bolster power generation during summer droughts, could partially mitigate the adverse effects on power generation.

Based on the data from 2006 to 2019, the solar PV and wind turbine fleets in the region displayed considerable resilience under the 2007 drought conditions. However, it is essential to recognize that this observation does not necessarily imply a consistent level of robustness for the VRE fleet in the future. This uncertainty arises due to the rapid integration of renewable energy sources within the region and the alterations in climate patterns driven by global warming. In the context of summer droughts, the simultaneous occurrence of wind drought is a distinct possibility. To gain a comprehensive understanding of the performance of VRE resources in the face of potential climate-induced extreme summer weather conditions in the future, further in-depth investigations are needed.

While this study exclusively assessed the effects of summer drought on the capacity of the generating fleet, it is essential to acknowledge that extreme weather events can have impacts extending well beyond power generation. Such events can significantly influence electricity demand and power transmission infrastructure. For instance, summer droughts typically lead to elevated temperatures, resulting in a surge in electricity demand and potential impacts on transmission capacity. For a thorough assessment of power system resilience under extreme drought conditions, future studies could aim to conduct a resilience analysis that integrates impact models encompassing generation, transmission, and load factors. This comprehensive approach will enable a more nuanced understanding of the system's resilience in the face of such extreme weather challenges. As highlighted by the sensitivity analysis, the continued reduction in streamflow and increasing air temperatures has a significant and adverse impact on the available capacity of both hydro and thermal generation fleets. Investigating the potential impacts of future climate-induced extreme drought events, which have the potential to be more severe than historical drought conditions, on available capacity of generation resources would be an intriguing area for research as well.

5. Conclusions

The objective of this paper was to quantify and understand the impacts of extreme summer drought on the available generating capacity of different generating technologies. To achieve this, a comprehensive and systematic framework for assessing the impact on generating capacity in bulk power systems was proposed, featuring high temporal and spatial resolution. This framework facilitates a thorough quantitative evaluation of usable generating capacity at the plant level, encompassing hydro, ON-based thermal, RC-based thermal, CT, and VRE, all at a daily time resolution. This paper also applied the framework to the real-world EI system, specifically the PJM and SERC regions with the near-term 2025 generation fleet, under a spectrum of summer weather conditions. Extensive real-world datasets were meticulously collected, encompassing historical hydrological and meteorological conditions, and various generator parameters. In total, the proposed framework for evaluating available capacity was employed for 6055 identified at-risk generators.

From this real-world case study, several key findings emerged. The available capacity distributions of individual generators under extreme summer conditions vary significantly, highlighting the necessity of plant-level derating modeling for precise capacity evaluations. It has been observed that hydrological and meteorological conditions had a relatively minor impact on thermal power plants equipped with RC cooling systems or CTs, especially when compared to hydro power plants and ON cooling based thermal power plants. Additionally, under the historical 2007 drought scenario, VRE displayed remarkable resilience in the face of elevated temperature and reduced precipitation. Overall, during drought periods resembling those in 2007, the total usable capacity of at-risk power plants in the region would experience a substantial decrease compared to a typical summer, falling within the range of 71% to 81% of the total installed capacity, potentially reaching as much as 8.5 GW across the entire fleet. The analysis also revealed that with every 10% reduction in streamflow compared to the 2007 summer drought conditions, the median available capacity of the hydro fleet would decrease by 1.40%.

It should be noted that this is the first paper that provides quantitative and systematic approaches showing the tangible effects of historical summer drought on the available generation capacity of the near-term PJM and SERC generation fleet based on publicly available real-world data sets. The case study results in this work can serve as a benchmark for future studies. Therefore, it has archival value for broad research communities in energy systems.

The contributions presented in this paper may motivate more extensive research aimed at comprehending the resilience of bulk power systems when confronted with the rigors of extreme drought conditions. Moreover, it is imperative to incorporate the observed impacts into the broader spectrum of power system long-term planning. This integration is pivotal for establishing a more comprehensive and integrated approach to evaluating power system performance. In the midst of an evolving climate landscape, insights derived from this study can guide policymakers, stakeholders, and operators in making informed decisions to enhance the power infrastructure and ensure its resilience in the face of potential extreme drought events and other environmental challenges.

CRediT authorship contribution statement

Hang Shuai: Writing – original draft, Validation, Software, Methodology, Investigation, Formal analysis, Data curation. **Fangxing Li:** Writing – review & editing, Validation, Supervision, Project administration, Methodology, Funding acquisition, Formal analysis, Conceptualization. **Jinxiang Zhu:** Writing – review & editing, Methodology, Data curation. **William Jerome Tingen II:** Writing – review & editing, Resources, Data curation. **Srijib Mukherjee:** Writing – review & editing, Funding acquisition, Conceptualization.

Declaration of competing interest

The authors declare that they have no known competing financial interests or personal relationships that could have appeared to influence the work reported in this paper.

Data availability

Data will be made available on request.

Acknowledgments

This work was supported in part by the U.S. DOE, Office of Energy Efficiency and Renewable Energy and Office of Electricity under Contract DE-AC05-00OR22725 and in part by the CURENT research center.

References

[1] Zhang J, Campana PE, Yao T, Zhang Y, Lundblad A, Melton F, Yan J. The water-food-energy nexus optimization approach to combat agricultural drought: a case study in the united states. Appl Energy 2018;227:449–64.
[2] Lubega WN, Stillwell AS. Maintaining electric grid reliability under hydrologic drought and heat wave conditions. Appl Energy 2018;210:538–49.
[3] Jones CB, Bresloff CJ, Darbali-Zamora R, Lave MS, Bezares EEA. Geospatial assessment methodology to estimate power line restoration access vulnerabilities after a hurricane in puerto rico. IEEE Open Access J Power Energy 2022;9:298–307.
[4] Lund J, Medellin-Azuara J, Durand J, Stone K. Lessons from california's 2012–2016 drought. J Water Resour Plan Manag 2018;144(10):04018067.
[5] Climate Change Institute UoM. Daily surface air temperature. 2023, Retrieved Jan. 2023, https://climatereanalyzer.org/.
[6] Yin J, Gentine P, Slater L, Gu L, Pokhrel Y, Hanasaki N, Guo S, Xiong L, Schlenker W. Future socio-ecosystem productivity threatened by compound drought–heatwave events. Nat Sustain 2023;6(3):259–72.
[7] Peer RA, Sanders KT. The water consequences of a transitioning us power sector. Appl Energy 2018;210:613–22.
[8] Su Y, Kern JD, Denaro S, Hill J, Reed P, Sun Y, Cohen J, Characklis GW. An open source model for quantifying risks in bulk electric power systems from spatially and temporally correlated hydrometeorological processes. Environ Model Softw 2020;126:104667.
[9] Shi Q, Liu W, Zeng B, Hui H, Li F. Enhancing distribution system resilience against extreme weather events: Concept review, algorithm summary, and future vision. Int J Electr Power Energy Syst 2022;138:107860.
[10] NERC. 2023 Summer reliability assessment. 2023, https://www.nerc.com/pa/RAPA/ra/Reliability%20Assessments%20DL/NERC_SRA_2023.pdf.
[11] Hart E, Mileva A. Advancing resource adequacy analysis with the gridpathra toolkit: A case study of the western us. Vol. 6, Energy Systems Integration Groups (ESIG) Webinar Presentation; 2022.
[12] NERC. Reliability assessments, https://www.nerc.com/pa/RAPA/ra/Pages/default.aspx.
[13] EPA. Resource adequacy analysis technical support document, https://www.epa.gov/system/files/documents/2023-05/Resource%20Adequacy%20Analysis%20TSD.pdf.
[14] ISO-NE. Qualified capacity for cso bilateral periods and reconfiguration auctions, https://www.iso-ne.com/markets-operations/markets/forward-capacity-market/fcm-participation-guide/qualified-capacity-post-fca.
[15] GridLAB. Gridpath ra toolkit, https://gridlab.org/gridpathratoolkit/.
[16] EIA. Drought effects on hydroelectricity generation in western u.s. differed by region in 2021. 2022, https://www.eia.gov/todayinenergy/detail.php?id=51839#::text=In%202021%2C%20a%20historic%20drought,average%20(2011%E2%80%932020).
[17] Voisin N, et al. Sensitivity of western us power system dynamics to droughts compounded with fuel price variability. Appl Energy 2019;247:745–54.
[18] Harto C, Yan Y, Demissie Y, Elcock D, Tidwell VC, Hallett K, Macknick J, Wigmosta M, Tesfa T. Analysis of drought impacts on electricity production in the western and texas interconnections of the United states. Tech. rep., Argonne National Lab.(ANL), Argonne, IL (United States); 2012.
[19] Turner SW, Voisin N, Nelson KD, Tidwell VC. Drought impacts on hydroelectric power generation in the western United states. Tech. rep., Pacific Northwest National Lab.(PNNL), Richland, WA (United States); 2022.
[20] Bartos MD, Chester MV. Impacts of climate change on electric power supply in the western united states. Nature Clim Change 2015;5(8):748–52.
[21] Eisner S. Comprehensive evaluation of the watergap3 model across climatic, physiographic, and anthropogenic gradients (Ph.D. thesis), 2016.
[22] Stanton MCB, Dessai S, Paavola J. A systematic review of the impacts of climate variability and change on electricity systems in europe. Energy 2016;109:1148–59.
[23] Wan W, Zhao J, Popat E, Herbert C, Döll P. Analyzing the impact of streamflow drought on hydroelectricity production: A global-scale study. Water Resour Res 2021;57(4):e2020WR028087.
[24] McCall J, Macknick J. Water-related power plant curtailments: an overview of incidents and contributing factors. Tech. rep., National Renewable Energy Lab.(NREL), Golden, CO (United States); 2016.
[25] EIA. U.s. electric power sector continues water efficiency gains. 2023, https://www.eia.gov/todayinenergy/detail.php?id=56820.
[26] Voisin N, Kintner-Meyer M, Skaggs R, Nguyen T, Wu D, Dirks J, Xie Y, Hejazi M. Vulnerability of the us western electric grid to hydro-climatological conditions: how bad can it get? Energy 2016;115:1–12.
[27] Qiu M, Ratledge N, Azevedo IML, Diffenbaugh NS, Burke M. Drought impacts on the electricity system, emissions, and air quality in the western united states. Proc Natl Acad Sci 2023;120(28):e2300395120. http://dx.doi.org/10.1073/pnas.2300395120.
[28] Förster H, Lilliestam J. Modeling thermoelectric power generation in view of climate change. Reg Environ Change 2010;10:327–38.
[29] Henry CL, Pratson LF. Differentiating the effects of climate change-induced temperature and streamflow changes on the vulnerability of once-through thermoelectric power plants. Environ Sci Technol 2019;53(7):3969–76.
[30] Huang J, Jones B, Thatcher M, Landsberg J. Temperature impacts on utility-scale solar photovoltaic and wind power generation output over australia under rcp 8.5. J Renew Sustain Energy 2020;12(4).
[31] Bloomfield H. Climate change, wind droughts and the implications for wind energy. 2021, https://energypost.eu/climate-change-wind-droughts-and-the-implications-for-wind-energy/.
[32] Cohen SM, Dyreson A, Turner S, Tidwell V, Voisin N, Miara A. A multi-model framework for assessing long-and short-term climate influences on the electric grid. Appl Energy 2022;317:119193.
[33] CNN. July hit a crucial warming threshold that scientists have warned the world should stay under, https://www.cnn.com/2023/08/08/world/july-climate-record-paris-agreement/index.html.
[34] FERC. Transmission system planning performance requirements for extreme weather. 2022, 87 fr 38020 https://www.federalregister.gov/documents/2022/06/27/2022-13471/transmission-system-planning-performance-requirements-for-extreme-weather.
[35] NPCC. Northeast power coordinating council reliability assessment for summer 2022, https://www.npcc.org/content/docs/public/library/reports/seasonal-assessment/2022/npcc-2022-summer-assessment.pdf.
[36] Howland E. Boosting transmission between east, west grids will lower costs: Nrel. 2021, https://www.utilitydive.com/news/transmission-east--west-seams-grids-lowers-costs-nrel-wind-solar/608475/.
[37] USGS. Usgs water data for the nation. 2023, https://waterdata.usgs.gov/nwis.
[38] NID. National inventory of dams. 2023, https://nid.sec.usace.army.mil/#/.
[39] EIA. Preliminary monthly electric generator inventory. 2022, https://www.eia.gov/electricity/data/eia860m/.
[40] EIA. Form eia-923 detailed data with previous form data. 2022, https://www.eia.gov/electricity/data/eia923/.
[41] Tennant DL. Instream flow regimens for fish, wildlife, recreation and related environmental resources. Fisheries 1976;1(4):6–10.
[42] EPA. Historical generation data. 2023, https://campd.epa.gov/data.
[43] Vaisala. Humidity conversion formulas, vaisala oyj. Tech. rep. b210973en-f, 2013, https://www.hatchability.com/Vaisala.pdf.
[44] Thornton M, Shrestha R, Wei Y, Thornton P, Kao S, Wilson B. Daymet: daily surface weather data on a 1-km grid for north america, version 4. Oak Ridge, Tennessee, Usa: Ornl Daac; 1840.
[45] De Sa A, Al Zubaidy S. Gas turbine performance at varying ambient temperature. Appl Therm Eng 2011;31(14–15):2735–9.
[46] Jabboury BG, Darwish MA. Performance of gas turbine co-generation power desalting plants under varying operating conditions in kuwait. Heat Recovery Syst CHP 1990;10(3):243–53.
[47] Huld T, Gottschalg R, Beyer HG, Topič M. Mapping the performance of pv modules, effects of module type and data averaging. Sol Energy 2010;84(2):324–38.
[48] Pfenninger S, Staffell I. Long-term patterns of european pv output using 30 years of validated hourly reanalysis and satellite data. Energy 2016;114:1251–65.
[49] Holmgren WF, Hansen CW, Mikofski MA. Pvlib python: A python package for modeling solar energy systems. J Open Source Softw 2018;3(29):884.
[50] NASA. Modern-era retrospective analysis for research and applications, version 2 (merra-2). 2022, https://gmao.gsfc.nasa.gov/reanalysis/MERRA-2/.
[51] Staffell I, Pfenninger S. Using bias-corrected reanalysis to simulate current and future wind power output. Energy 2016;114:1224–39.
[52] Heddinghaus T. U.s drought monitor data from cpc/noaa, https://droughtmonitor.unl.edu/Maps/MapArchive.aspx.
[53] Copernicus. Low winds. 2021, https://climate.copernicus.eu/esotc/2021/low-winds.
[54] SWAT. Soil & water assessment tool, https://swat.tamu.edu/.
[55] Uría-Martínez R, Johnson MM, Shan R, Samu NM, Oladosu G, Werble JM, Battey H. Us hydropower market report. Tech. rep., Oak Ridge National Lab.(ORNL), Oak Ridge, TN (United States); 2021.